Available online at www.sciencedirect.com

ScienceDirect

Nuclear Physics B 931 (2018) 469–505

NUCLEAR PHYSICS B

www.elsevier.com/locate/nuclphysb

Consistency of perturbed tribimaximal, bimaximal and democratic mixing with neutrino mixing data

Sumit K. Garg

Department of Physics, CMR University, Bengaluru 562149, India

Received 14 February 2018; accepted 10 April 2018
Available online 25 May 2018
Editor: Hong-Jian He

Abstract

We scrutinize corrections to tribimaximal (TBM), bimaximal (BM) and democratic (DC) mixing matrices for explaining recent global fit neutrino mixing data. These corrections are parameterized in terms of small orthogonal rotations (R) with corresponding modified PMNS matrices of the forms $\left(R^l_{ij}\cdot U,\ U\cdot R^r_{ij},\ U\cdot R^r_{ij}\cdot R^r_{kl},\ R^l_{ij}\cdot R^l_{kl}\cdot U\right)$ where $R^{l,r}_{ij}$ is rotation in ij sector and U is any one of these special matrices. We showed that for perturbative schemes dictated by single rotation, only $\left(R^l_{12}\cdot U_{BM},\ R^l_{13}\cdot U_{BM},\ U_{TBM}\cdot R^r_{13}\right)$ can fit the mixing data at 3σ level. However for $R^l_{ij}\cdot R^l_{kl}\cdot U$ type rotations, only $\left(R^l_{23}\cdot R^l_{13}\cdot U_{DC}\right)$ is successful to fit all neutrino mixing angles within 1σ range. For $U\cdot R^r_{ij}\cdot R^r_{kl}$ perturbative scheme, only $\left(U_{BM}\cdot R^r_{12}\cdot R^r_{13},\ U_{DC}\cdot R^r_{12}\cdot R^r_{23},\ U_{TBM}\cdot R^r_{12}\cdot R^r_{13}\right)$ are consistent at 1σ level. The remaining double rotation cases are either excluded at 3σ level or successful in producing mixing angles only at $2\sigma-3\sigma$ level. We also updated our previous analysis on PMNS matrices of the form $\left(R_{ij}\cdot U\cdot R_{kl}\right)$ with recent mixing data. We showed that the results modifies substantially with fitting accuracy level decreases for all of the permitted cases except $\left(R_{12}\cdot U_{BM}\cdot R_{13},\ R_{23}\cdot U_{TBM}\cdot R_{13}\right.$ and $\left.R_{13}\cdot U_{TBM}\cdot R_{13}\right)$ in this rotation scheme.

E-mail address: sumit.k@cmr.edu.in.

https://doi.org/10.1016/j.nuclphysb.2018.04.022

1. Introduction

The Standard Model (SM) which governs the dynamics of interactions between fundamental particles contain massless neutrinos. But now its well established fact from the solar, atmospheric and reactor neutrino experiments [1–5] that neutrino switches flavor while traveling because of their tiny mass and flavor mixing. Thus its a clear evidence of Physics Beyond Standard Model. The understanding of extremely small neutrino mass ($\sim$ meV) and magnitude of mixing among different neutrino flavors are much deliberated issues in Particle Physics. The smallness of neutrino mass scale is well explained by seesaw mechanism [6] which links it to a new physical scale in Nature. However neutrino mixing indicate interesting pattern in which two mixing angles of a three flavor scenario seems to be maximal while third one remains small. Different mixing schemes like tribimaximal (TBM) [7], bimaximal (BM) [8] and democratic mixing (DC) [9] were explored to explain experimental neutrino mixing data. All these mixing scenarios have same predictions for the reactor mixing angle viz $\theta_{13} = 0$. The atmospheric mixing angle, $\theta_{23} = 45°$ for BM and TBM while for DC it takes the value 54.7°. The solar mixing angle is maximal (i.e. 45°) for BM and DC while takes the value of 35.3° for TBM mixing. As far origin of these special structures is concerned they can easily come from various discrete symmetries like A_4 [10], S_4 [11] etc. These issues are extensively discussed in literature.

However, reactor based Daya Bay [1] experiment in China presented first conclusive result of non zero θ_{13} using $\bar{\nu}_e$ beam with corresponding significance of 5.2σ. The value of 1–3 mixing angle consistent with data at 90% CL is reported to be in the range $\sin^2 2\theta_{13} = 0.092 \pm 0.016(stat) \pm 0.05(syst)$. Previously long baseline neutrino oscillation T2K experiment [2] observed the events corresponding to $\nu_\mu \to \nu_e$ transition which is also consistent with non zero θ_{13} in a three flavor scenario. The value of 1–3 mixing angle consistent with data at 90% CL is reported to be in the range $5°(5.8°) < \theta_{13} < 16°(17.8°)$ for Normal (Inverted) neutrino mass hierarchy. These results go in well agreement with other oscillation experiments like Double Chooz [3], Minos [4] and RENO [5]. Moreover it is evident from recent global fit [12,13] for neutrino masses and mixing angles (given in Table 2) that these mixing scenarios can't be taken at their face value and thus should be investigated for possible perturbations. This issue has been taken up many times [14,15] in literature. In particular, ref. [16] and ref. [17] discussed the perturbations that are parametrized in terms of mixing angles to DC and TBM mixing respectively for obtaining large θ_{13}. Here we looked into possible perturbations which are parameterized by one and two rotation matrices and are of the forms $\left(R_{ij} \cdot U, U \cdot R_{ij}, R_{ij} \cdot R_{kl} \cdot U, U \cdot R_{ij} \cdot R_{kl}\right)$. These corrections show strong correlations among neutrino mixing angles which are weakened with full perturbation matrix. Since the form of PMNS matrix is given by $U_{PMNS} = U_l^\dagger U_\nu$ so these modifications may originate from charged lepton and neutrino sector respectively. Unlike previous studies [16–18], we used χ^2 approach [19] to investigate the situation of mixing angle fitting in parameter space and thus capture essential information about corresponding correction parameters. Also to study correlations among neutrino mixing angles, we allowed to vary all mixing angles in their permissible limits instead of fixing one of them at a particular value to study correlation between remaining two mixing angles. This in our view show a full picture and thus we present our results in terms of 2 dimensional scatter plots instead of line plots [18]. Moreover we confined ourselves to small rotation limit which in turn justify them to pronounce as perturbative corrections. We also looked into new cases apart from the ones that were presented in [18] and thus presenting a complete analysis on these rotation schemes. Here we also take opportunity to update our previous analysis [19] on $\left(R_{ij} \cdot U \cdot R_{kl}\right)$ PMNS matrix for new mixing data. We find (χ^2_{min}, Best fit level) for different mixing cases [19] using

previous mixing data [12] and compare it with the results that are obtained with new mixing data [13]. In this study, we work in CP conserving limit and thus all phases are taken to be zero. However we would like to emphasize that CP violation can have a deep impact on these studies. But including CP violation for the characterized perturbations is a elaborative task which in our opinion needs separate attention. So we leave the discussion of corrections coming from non zero CP phase for future investigations. These results can help in understanding the structure of corrections that these well known mixing scenarios require in order to be consistent with neutrino mixing data. Thus this study may turn out to be useful in restricting vast number of possible models which offers different corrections to these mixing schemes in neutrino model building physics. It would also be interesting to inspect the origin of these perturbations in a model dependent framework. However the investigation of all such issues is left for future consideration.

The main outline of the paper is as follows. In section 2, we will give general discussion about our work. In sections 3–7, we will present our numerical results for various possible perturbation cases. Finally in section 8, we will give the summary and conclusions of our study.

2. General setup

A 3×3 Unitary matrix can be parametrized by 3 mixing angles and 6 phases. However 5 phases can be moved away leaving behind only 1 physical phase. Thus light neutrino mixing is given in standard form as [20]

$$U = \begin{pmatrix} 1 & 0 & 0 \\ 0 & c_{23} & s_{23} \\ 0 & -s_{23} & c_{23} \end{pmatrix} \begin{pmatrix} c_{13} & 0 & s_{13}e^{-i\delta} \\ 0 & 1 & 0 \\ -s_{13}e^{i\delta} & 0 & c_{13} \end{pmatrix} \begin{pmatrix} c_{12} & s_{12} & 0 \\ -s_{12} & c_{12} & 0 \\ 0 & 0 & 1 \end{pmatrix} \begin{pmatrix} 1 & 0 & 0 \\ 0 & e^{i\rho} & 0 \\ 0 & 0 & e^{i\sigma} \end{pmatrix}, \tag{2.1}$$

where $c_{ij} \equiv \cos\theta_{ij}$, $s_{ij} \equiv \sin\theta_{ij}$ and δ is the Dirac CP violating phase. Here two additional phases ρ and σ are only pertinent if neutrinos turn out to be Majorana particles. The Majorana phases however do not affect the neutrino oscillations and thus are not relevant here. In this study, we will consider the case where all the CP violating phases i.e. δ, ρ, σ are zero. The effects of CP violation will be discussed somewhere else.

The form of mixing matrix for the three mixing scenarios under consideration is given as follows:

$$U_{\rm TBM} = \begin{pmatrix} \sqrt{\frac{2}{3}} & \sqrt{\frac{1}{3}} & 0 \\ -\sqrt{\frac{1}{6}} & \sqrt{\frac{1}{3}} & \sqrt{\frac{1}{2}} \\ -\sqrt{\frac{1}{6}} & \sqrt{\frac{1}{3}} & -\sqrt{\frac{1}{2}} \end{pmatrix}, \quad U_{\rm BM} = \begin{pmatrix} \sqrt{\frac{1}{2}} & \sqrt{\frac{1}{2}} & 0 \\ -\frac{1}{2} & \frac{1}{2} & \sqrt{\frac{1}{2}} \\ \frac{1}{2} & -\frac{1}{2} & \sqrt{\frac{1}{2}} \end{pmatrix},$$

$$U_{\rm DC} = \begin{pmatrix} \sqrt{\frac{1}{2}} & \sqrt{\frac{1}{2}} & 0 \\ \sqrt{\frac{1}{6}} & -\sqrt{\frac{1}{6}} & -\sqrt{\frac{2}{3}} \\ -\sqrt{\frac{1}{3}} & \sqrt{\frac{1}{3}} & -\sqrt{\frac{1}{3}} \end{pmatrix}.$$

The resulting value of mixing angles from above matrices is given in Table 1. All of them predict vanishing value of $\theta_{13} = 0°$. The atmospheric mixing angle (θ_{23}) is maximal in TBM

Table 1
Mixing angle values from special matrices. All angles are in degrees (θ°).

Mixing angle	Bimaximal (BM)	Democratic (DC)	Tribimaximal (TBM)
θ_{23}°	45	54.7	45
θ_{12}°	45	45	35.3
θ_{13}°	0	0	0

Table 2
Three-flavor oscillation neutrino mixing angles from fit to global data [13]. All mixing angles are in degrees (θ°).

Neutrino mixing angle (θ°)	Normal Hierarchy (NH)			
	Best fit	1σ	2σ	3σ
θ_{12}°	33.02	32.01–34.08	30.98–35.30	30.0–36.51
θ_{23}°	40.68	39.81–41.9	38.93–43.28	38.11–51.64
θ_{13}°	8.43	8.29–8.56	8.10–8.74	7.92–8.91

and BM scenarios while it takes the larger value of 54.7° for DC mixing. The value of solar mixing angle (θ_{12}) is maximal in BM and DC scenarios while its value is 35.3° for TBM case. However these mixing angles are in conflict with recent experimental observations which provide best fit values at $\theta_{13} \sim 8^\circ$, $\theta_{12} \sim 33^\circ$ and $\theta_{23} \sim 41^\circ$. Thus these well studied structures need corrections [21–23] in order to be consistent with current neutrino mixing data.

From theoretical point of view, neutrino mixing matrix U comes from the mismatch between diagonalization of charged lepton and neutrino mass matrix and is given as

$$U = U_l^\dagger U_\nu$$

where U_l and U_ν are the unitary matrices that diagonalizes the charged lepton (M_l) and neutrino mass matrix (M_ν). Thus corrections that can modify the original predictions of above special structures can originate from following sources.

(i) Charged lepton sector i.e. $U'_{PMNS} = U^l_{crr} \cdot U_{PMNS}$
(ii) Neutrino sector i.e. $U'_{PMNS} = U_{PMNS} \cdot U^\nu_{crr}$
(iii) Both sectors i.e. $U'_{PMNS} = U^l_{crr} \cdot U_{PMNS} \cdot U^\nu_{crr}$

Here U^l_{crr} and U^ν_{crr} are the correction matrices corresponding to charged lepton and neutrino sector respectively. For CP conserving case, U^l_{crr} and U^ν_{crr} are the real orthogonal matrices which can be parametrized in terms of 3 mixing angles as discussed previously.

In this study, we are considering first two cases i.e. possible modifications that comes from charged lepton and neutrino sector. The 3rd case is already investigated [19] in detail before. We tested different possibilities for fitting neutrino mixing data that are governed by either one or two mixing angles of perturbation matrix. These cases exhibit strong correlations among mixing angles which are weakened or hidden in situation where all angles are non zero. Here corresponding PMNS matrix is of the forms $R_X \cdot U$, $U \cdot R_X$, $R_X \cdot R_Y \cdot U$ and $U \cdot R_X \cdot R_Y$ where R_X and R_Y denote generic perturbation matrices and U is any of these special matrix. The perturbation matrices R_X and R_Y can be expressed in terms of mixing matrices as $R_X(R_Y) = \{R_{23}, R_{13}, R_{12}\}$

in general, where R_{23}, R_{13} and R_{12} represent the rotations in 23, 13 and 12 sector respectively and are given by

$$R_{12} = \begin{pmatrix} \cos\alpha & \sin\alpha & 0 \\ -\sin\alpha & \cos\alpha & 0 \\ 0 & 0 & 1 \end{pmatrix}, \quad R_{23} = \begin{pmatrix} 1 & 0 & 0 \\ 0 & \cos\beta & \sin\beta \\ 0 & -\sin\beta & \cos\beta \end{pmatrix},$$

$$R_{13} = \begin{pmatrix} \cos\gamma & 0 & \sin\gamma \\ 0 & 1 & 0 \\ -\sin\gamma & 0 & \cos\gamma \end{pmatrix}$$

where α, β, γ denote rotation angles. The corresponding PMNS matrix for single rotation case is given by:

$$U_{\alpha\beta}^{TBML} = R_{\alpha\beta}^{l} \cdot U_{TBM}\,, \tag{2.2}$$

$$U_{\alpha\beta}^{BML} = R_{\alpha\beta}^{l} \cdot U_{BM}\,, \tag{2.3}$$

$$U_{\alpha\beta}^{DCL} = R_{\alpha\beta}^{l} \cdot U_{DC}\,, \tag{2.4}$$

and

$$U_{\alpha\beta}^{TBMR} = U_{TBM} \cdot R_{\alpha\beta}^{r}\,, \tag{2.5}$$

$$U_{\alpha\beta}^{BMR} = U_{BM} \cdot R_{\alpha\beta}^{r}\,, \tag{2.6}$$

$$U_{\alpha\beta}^{DCR} = U_{DC} \cdot R_{\alpha\beta}^{r}\,, \tag{2.7}$$

where $(\alpha\beta) = (12), (13), (23)$ respectively. The corresponding PMNS matrix for two rotation matrix thus becomes:

$$U_{\text{ijkl}}^{TBML} = R_{ij}^{l} \cdot R_{kl}^{l} \cdot U_{TBM}\,, \tag{2.8}$$

$$U_{\text{ijkl}}^{BML} = R_{ij}^{l} \cdot R_{kl}^{l} \cdot U_{BM}\,, \tag{2.9}$$

$$U_{\text{ijkl}}^{DCL} = R_{ij}^{l} \cdot R_{kl}^{l} \cdot U_{DC}\,, \tag{2.10}$$

and

$$U_{\text{ijkl}}^{TBMR} = U_{TBM} \cdot R_{ij}^{r} \cdot R_{kl}^{r}\,, \tag{2.11}$$

$$U_{\text{ijkl}}^{BMR} = U_{BM} \cdot R_{ij}^{r} \cdot R_{kl}^{r}\,, \tag{2.12}$$

$$U_{\text{ijkl}}^{DCR} = U_{DC} \cdot R_{ij}^{r} \cdot R_{kl}^{r}\,, \tag{2.13}$$

where $(ij), (kl) = (12), (13), (23)$ respectively. Now to get neutrino mixing angles the above matrices are compared with the standard PMNS matrix.

To investigate numerically the effect of these perturbations we define a χ^2 function which is a measure of deviation from the central value of mixing angles:

$$\chi^2 = \sum_{i=1}^{3} \{\frac{\theta_i(P) - \theta_i}{\delta\theta_i}\}^2 \tag{2.14}$$

with $\theta_i(P)$ are the theoretical value of mixing angles which are functions of perturbation parameters (α, β, γ). θ_i are the experimental value of neutrino mixing angles with corresponding

Table 3
χ^2 value for Normal Hierarchy (NH) with different unperturbed mixing schemes.

χ^2_{NH}		
Bimaximal (BM)	Democratic (DC)	Tribimaximal (TBM)
1112.0	1274.9	965.5

1σ uncertainty $\delta\theta_i$. The corresponding value of χ^2 for different mixing schemes is given in Table 3.

We investigated the role of various possible perturbations for lowering the value of χ^2 from its original prediction in different mixing schemes. A good numerical fit should produce low χ^2 value in parameter space.

3. Numerical results

In this section, we will discuss numerical findings of our study for Normal Hierarchy. We studied the role of various perturbative schemes in producing large θ_{13} [14] and fitting other mixing angles. In Figs. 1–50, we present the results in terms of χ^2 over perturbation parameters and θ_{13} over $\theta_{23} - \theta_{12}$ plane for various studied cases. For performing numerical study, we used exact expressions of modified mixing angles in terms of correction parameters. However in relevant sections we present approximate form of these expressions that will reveal about the nature of corrections. This in turn will give information about the size of deviation a mixing angle can have in parameter space from its unperturbed value.

The numerical value of correction parameters α, β and γ are confined in the range $[-0.5, 0.5]$ so as to keep them in perturbative limits. We enforced the condition $\chi^2 < \chi^2_i$ (i = TBM, DC and BM) for plotting data points. In double rotation plots of χ^2 vs perturbation parameters (θ_1, θ_2) red, blue and light green color regions corresponds to χ^2 value in the interval $[0, 3]$, $[3, 10]$ and > 10 respectively. The white region of plot corresponds to completely disallowed part of $\chi^2 > \chi^2_{unperturbed}$. In figures of neutrino mixing angles, light green band corresponds to 1σ and full color band to 3σ values of θ_{13}. Also '$\times$' refers to the case which is unable to fit mixing angles even at 3σ level while '–' denotes the situation where $\theta_{13} = 0$. In order to show the correlations between left and right figures we marked the $\chi^2 < 3, [3, 10]$ regions in mixing angle plots with different color codings. The white region corresponds to $3 < \chi^2 < 10$ while yellow region belongs to $\chi^2 < 3$. Horizontal and vertical dashed black, dashed pink and thick black lines corresponds to 1σ, 2σ and 3σ ranges of the other two mixing angles. Now we will take up the case of various possible forms of rotations one by one.

4. Rotations-$R^l_{ij}.U$

Here we first consider the perturbations for which the form of modified PMNS matrix is given by $U_{PMNS} = R^l_{ij}.U$. We will investigate their role in fitting the neutrino mixing angles.

4.1. 12 rotation

This case corresponds to rotation in 12 sector of these special matrices. Since for small rotation $\sin\theta \approx \theta$ and $\cos\theta \approx 1 - \theta^2$, so the neutrino mixing angles truncated at order O (θ^2) for this rotation are given by

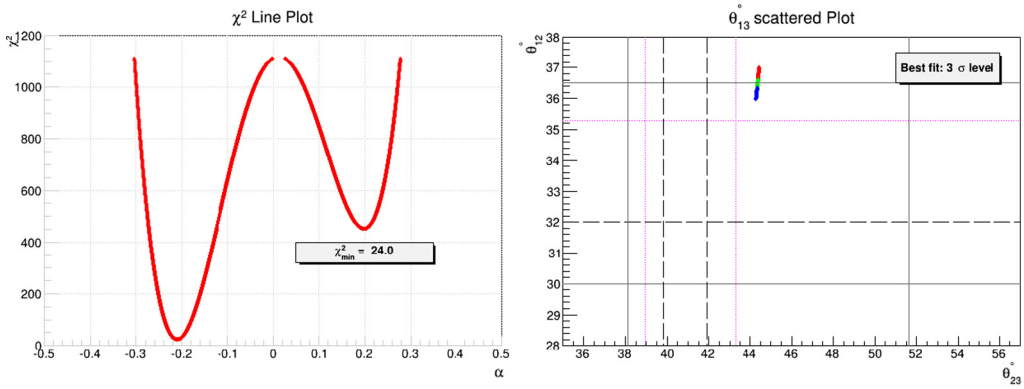

Fig. 1. Line plot of χ^2 (left fig.) vs α (in radians) and scattered plot of θ_{13} (right fig.) over $\theta_{23} - \theta_{12}$ (in degrees) plane for U_{12}^{BML} rotation scheme. The discontinuity in left curve corresponds to region where $\chi^2_{perturbed} > \chi^2_{original}$. The information about other color coding and various horizontal, vertical lines in right fig. is given in text. (For interpretation of the colors in the figure(s), the reader is referred to the web version of this article.)

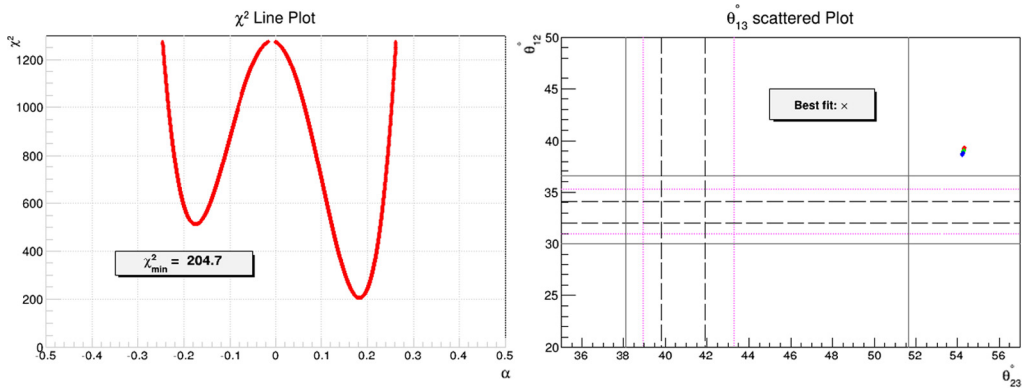

Fig. 2. Line plot of χ^2 (left fig.) vs α (in radians) and scattered plot of θ_{13} (right fig.) over $\theta_{23} - \theta_{12}$ (in degrees) plane for U_{12}^{DCL} rotation scheme.

$$\sin\theta_{13} \approx |\alpha U_{23}|, \tag{4.1}$$

$$\sin\theta_{23} \approx |\frac{(\alpha^2 - 1)U_{23}}{\cos\theta_{13}}|, \tag{4.2}$$

$$\sin\theta_{12} \approx |\frac{U_{12} + \alpha U_{22} - \alpha^2 U_{12}}{\cos\theta_{13}}|. \tag{4.3}$$

Figs. 1–3 show the numerical results corresponding to TBM, BM and DC case. The salient features of this mixing is given by:

(i) The atmospheric mixing angle (θ_{23}) receive corrections only of $O(\theta^2)$ so its perturbed value remain close to its original prediction.

(ii) In BM, for fitting θ_{13} in its 3σ range constraints $|\alpha| \in [0.196, 0.220]$ which in turn fixes $\theta_{12} \in [35.97°, 36.99°]$ for negative and $\theta_{12} \in [53.0°, 54.02°]$ for positive α region. The atmospheric angle (θ_{23}) remain confined to very narrow range $\theta_{23} \in [44.29°, 44.44°]$ for

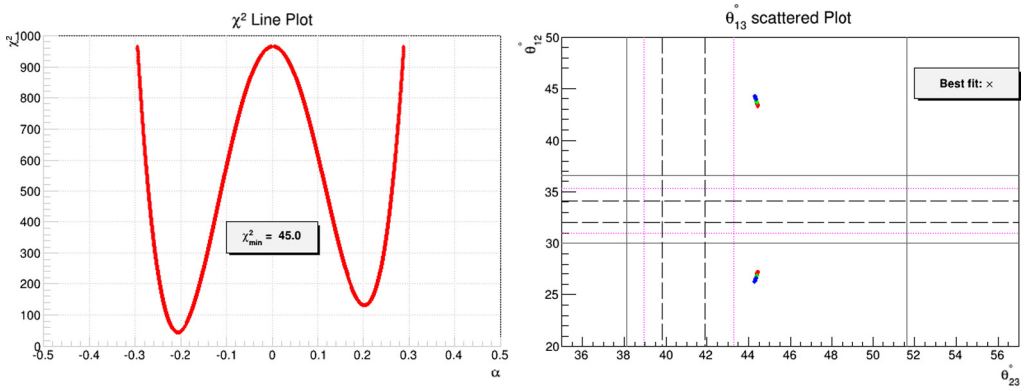

Fig. 3. Line plot of χ^2 (left fig.) vs α (in radians) and scattered plot of θ_{13} (right fig.) over $\theta_{23} - \theta_{12}$ (in degrees) plane for U_{12}^{TBML} rotation scheme.

mentioned value of α. Thus negative α is preferred and it can fit all mixing angles at 3σ level.

(iii) However same window of α for TBM (since U_{23} is same in both cases) gives low (high) value of θ_{12} for its negative (positive) range. These achieved values are well away from their allowed 3σ boundary. In DC case, $|\alpha| \in [0.169, 0.190]$ for setting θ_{13} in its 3σ range which in turn fixes θ_{12} away from its allowed 3σ range.

(iv) The minimum value of $\chi^2 \sim 24.0$, 204.7 and 45.0 for BM, DC and TBM case respectively.

(v) The perturbed BM is consistent at 3σ level and gives $\theta_{12} \sim 36.39°$, $\theta_{23} \sim 44.35°$ and $\theta_{13} \sim 8.51°$ for its respective best fit. The other two cases are not favored.

4.2. 13 rotation

This case pertains to rotation in 13 sector of these special matrices. The neutrino mixing angles for small perturbation parameter γ are given by

$$\sin\theta_{13} \approx |\gamma U_{33}|, \tag{4.4}$$

$$\sin\theta_{23} \approx |\frac{U_{23}}{\cos\theta_{13}}|, \tag{4.5}$$

$$\sin\theta_{12} \approx |\frac{U_{12} + \gamma U_{32} - \gamma^2 U_{12}}{\cos\theta_{13}}|. \tag{4.6}$$

Figs. 4–6 show the numerical results corresponding to TBM, BM and DC case. The main features of this perturbative scheme are given by

(i) Here atmospheric mixing angle (θ_{23}) receives only minor corrections through $\sin\theta_{13}$ and thus its value doesn't change much from its original prediction.

(ii) In BM case, for fitting θ_{13} in its 3σ range constraints $|\gamma| \in [0.196, 0.220]$ which in turn fixes $\theta_{12} \in [35.97°, 36.99°]$ for positive and $\theta_{12} \in [53.0°, 54.02°]$ for its negative range. The corresponding θ_{23} remains close to its original prediction in the range $\theta_{23} \in [45.55°, 45.70°]$.

(iii) However same range of $|\gamma|$ for TBM since $|U_{33}|$ is same in both cases gives θ_{12} well away from its allowed 3σ range. In DC case, $|\gamma| \in [0.241, 0.271]$ for θ_{13} to be in its 3σ range

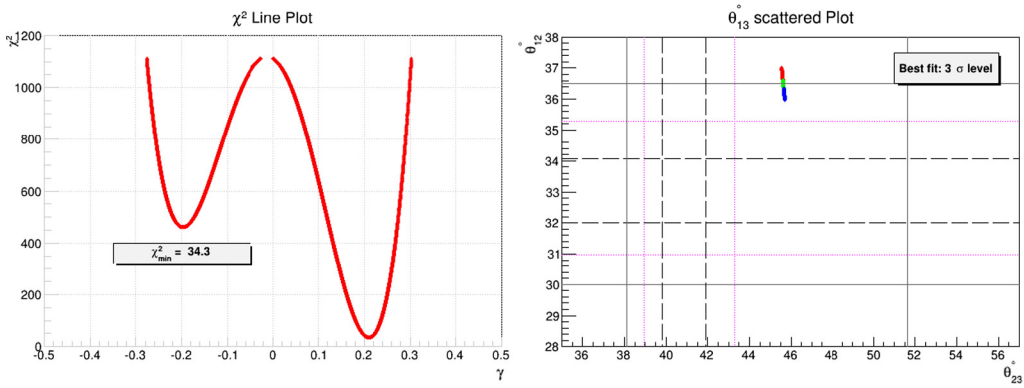

Fig. 4. Line plot of χ^2 (left fig.) vs γ (in radians) and scattered plot of θ_{13} (right fig.) over $\theta_{23} - \theta_{12}$ (in degrees) plane for U_{13}^{BML} rotation scheme.

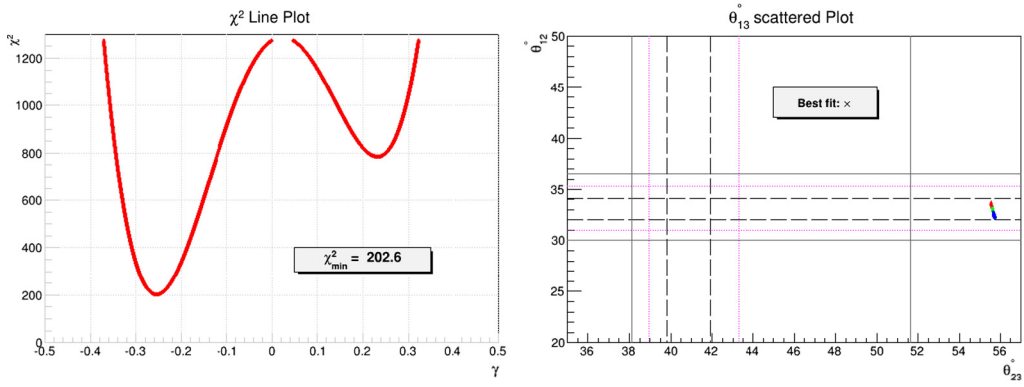

Fig. 5. Line plot of χ^2 (left fig.) vs γ (in radians) and scattered plot of θ_{13} (right fig.) over $\theta_{23} - \theta_{12}$ (in degrees) plane for U_{13}^{DCL} rotation scheme.

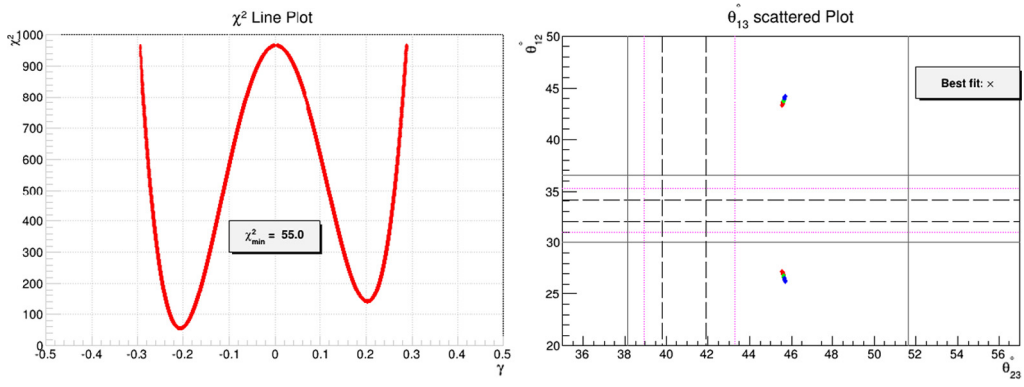

Fig. 6. Line plot of χ^2 (left fig.) vs γ (in radians) and scattered plot of θ_{13} (right fig.) over $\theta_{23} - \theta_{12}$ (in degrees) plane for U_{13}^{TBML} rotation scheme.

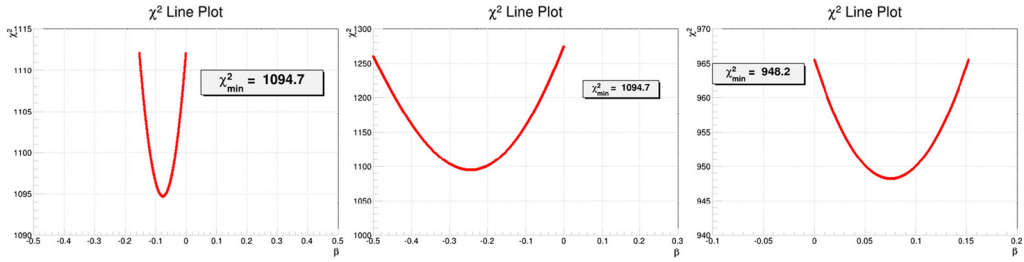

Fig. 7. Line plot of χ^2 (left fig.) vs γ (in radians) for U_{23}^{BML}, U_{23}^{DCL} and U_{23}^{TBML} rotation scheme.

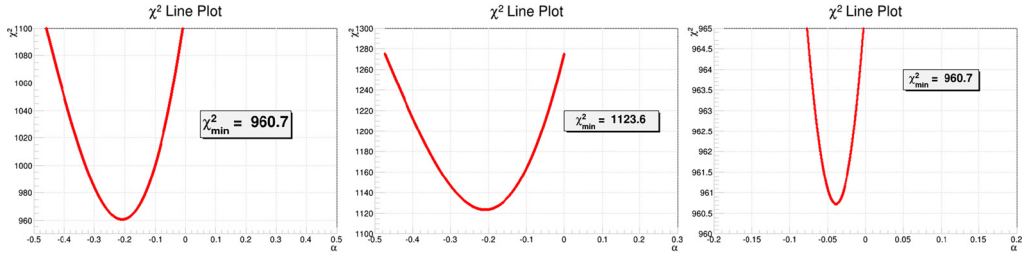

Fig. 8. Line plot of χ^2 (left fig.) vs γ (in radians) for U_{12}^{BMR}, U_{12}^{DCR} and U_{12}^{TBMR} rotation scheme.

which fixes $\theta_{12} \in [56.34°, 57.78°]$ for +ve values of γ and $\theta_{12} \in [32.21°, 33.65°]$ for its −ve range. Thus negative γ is preferred but this in turn puts $\theta_{23} \in [55.52°, 55.73°]$ which is well away from its allowed 3σ range.

(iv) The minimum value of $\chi^2 \sim 34.3$, 202.6 and 55.0 for BM, DC and TBM case respectively.

(v) The BM case is consistent at 3σ level and produces $\theta_{12} \sim 36.42°$, $\theta_{23} \sim 45.63°$ and $\theta_{13} \sim 8.48°$ for its corresponding best fit. The other two cases are not viable.

4.3. 23 rotation

In this case, θ_{13} doesn't receive any corrections from perturbation matrix (i.e. $\theta_{13} = 0$) and the minimum value of $\chi^2 \sim 1094.7$, 1094.7 and 948.2 for BM, DC and TBM case respectively. Thus we left out this case for any further discussion.

5. Rotations-$U.R_{ij}^r$

Here we first consider the perturbations for which modified PMNS matrix is given by $U_{PMNS} = R_{ij}^r.U$. We will investigate the role of these perturbations in fitting the neutrino mixing data.

5.1. 12 rotation

This case pertains to the situation where $\theta_{13} = 0$ and the minimum value of $\chi^2 \sim 960.7$, 1123.6 and 960.7 for BM, DC and TBM case respectively. Thus we haven't investigated it any further.

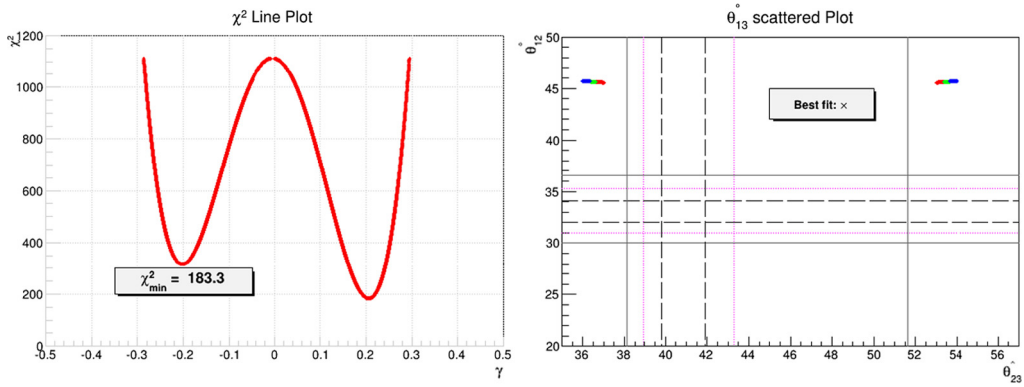

Fig. 9. Line plot of χ^2 (left fig.) vs γ (in radians) and scattered plot of θ_{13} (right fig.) over $\theta_{23} - \theta_{12}$ (in degrees) plane for U_{13}^{BMR} rotation scheme.

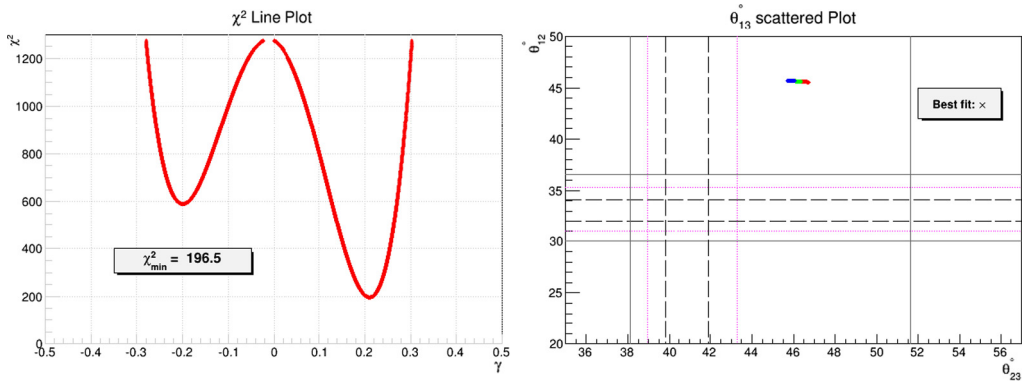

Fig. 10. Line plot of χ^2 (left fig.) vs γ (in radians) and scattered plot of θ_{13} (right fig.) over $\theta_{23} - \theta_{12}$ (in degrees) plane for U_{13}^{DCR} rotation scheme.

5.2. 13 rotation

This case corresponds to rotation in 13 sector of these special matrices. The mixing angles for small perturbation parameter γ are given by

$$\sin\theta_{13} \approx |\gamma U_{11}|, \tag{5.1}$$

$$\sin\theta_{23} \approx |\frac{U_{23} + \gamma U_{21} - \gamma^2 U_{23}}{\cos\theta_{13}}|, \tag{5.2}$$

$$\sin\theta_{12} \approx |\frac{U_{12}}{\cos\theta_{13}}|. \tag{5.3}$$

Figs. 9–11 show the numerical results corresponding to TBM, BM and DC case. The main features of these corrections are given as:

(i) Here solar mixing angle (θ_{12}) receives only small corrections through $\sin\theta_{13}$ and thus its value remain close to its original prediction.

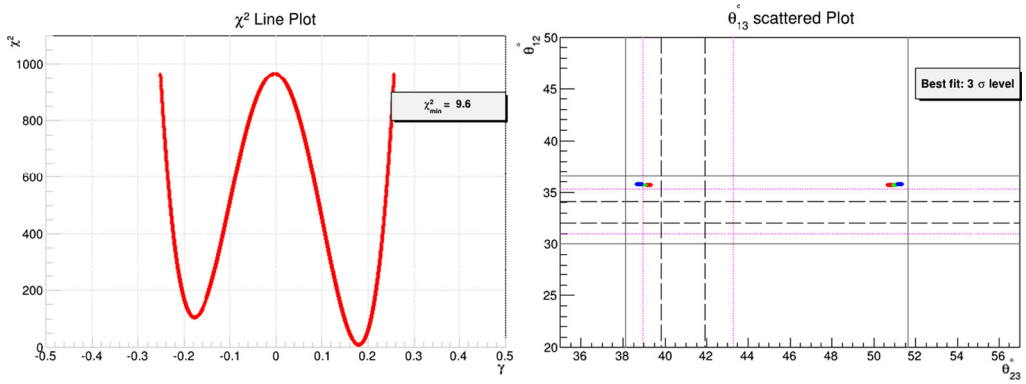

Fig. 11. Line plot of χ^2 (left fig.) vs γ (in radians) and scattered plot of θ_{13} (right fig.) over $\theta_{23} - \theta_{12}$ (in degrees) plane for U_{13}^{TBMR} rotation scheme.

(ii) In TBM case, for fitting θ_{13} in its 3σ range constraints $|\gamma| \in [0.169, 0.190]$ which in turn fixes $\theta_{23} \in [38.63°, 39.35°]$ for positive and $\theta_{23} \in [50.64°, 51.36°]$ for its negative range. The solar mixing angle (θ_{12}) remains confined in the narrow range $\theta_{12} \in [35.65°, 35.76°]$. Thus positive as well as negative γ regions are allowed.

(iii) However for BM and DC, we require $|\gamma| \in [0.196, 0.220]$ to fit θ_{13} in its 3σ range. But said range drives θ_{12} well away from its allowed 3σ range.

(iv) The minimum value of $\chi^2 \sim 183.3$, 196.5 and 9.6 for BM, DC and TBM case respectively.

(v) The TBM case is consistent at 3σ level and produces $\theta_{12} \sim 35.70°$, $\theta_{23} \sim 39.0°$ and $\theta_{13} \sim 8.40°$ for its best fit. The other two cases are not viable.

5.3. 23 rotation

This case corresponds to rotation in 23 sector of these special matrices. The neutrino mixing angles for small rotation parameter β are given by

$$\sin\theta_{13} \approx |\beta U_{12}|, \tag{5.4}$$

$$\sin\theta_{23} \approx |\frac{U_{23} + \beta U_{22} - \beta^2 U_{23}}{\cos\theta_{13}}|, \tag{5.5}$$

$$\sin\theta_{12} \approx |\frac{(\beta^2 - 1)U_{12}}{\cos\theta_{13}}|. \tag{5.6}$$

Figs. 12–14 show the numerical results corresponding to TBM, BM and DC case. The salient features in this perturbative scheme are given by:

(i) The atmospheric mixing angle (θ_{12}) receives corrections only of the $O(\theta^2)$ so its value remains close to its original prediction.

(ii) In TBM case, for fitting θ_{13} in its 3σ range constraints $|\beta| \in [0.241, 0.271]$ which in turn fixes $\theta_{23} \in [56.34°, 57.78°]$ for positive and $\theta_{23} \in [32.21°, 33.65°]$ for its negative range. However solar mixing angle (θ_{12}) lies close to its original prediction $\theta_{12} \in [34.26°, 34.47°]$. Thus this case is ruled out at 3σ level.

(iii) However for BM and DC, we require $|\beta| \in [0.196, 0.220]$ to fit θ_{13} in its 3σ range. But said range drives θ_{12} well away from its allowed 3σ range.

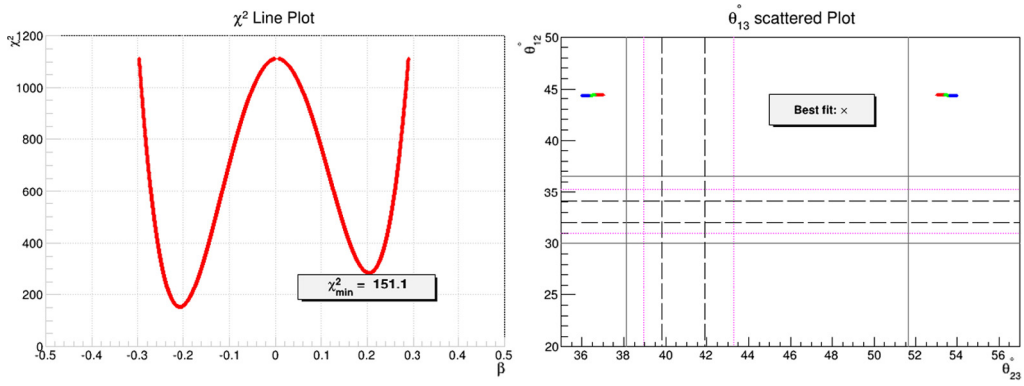

Fig. 12. Line plot of χ^2 (left fig.) vs β (in radians) and scattered plot of θ_{13} (right fig.) over $\theta_{23} - \theta_{12}$ (in degrees) plane for U_{23}^{BMR} rotation scheme.

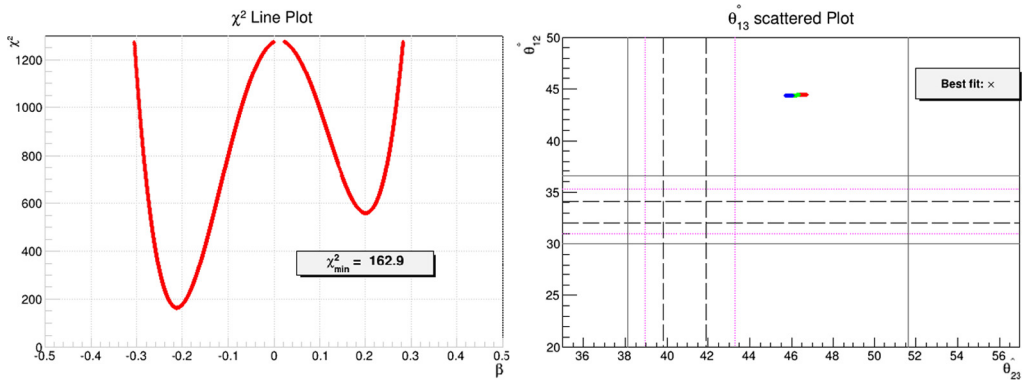

Fig. 13. Line plot of χ^2 (left fig.) vs β (in radians) and scattered plot of θ_{13} (right fig.) over $\theta_{23} - \theta_{12}$ (in degrees) plane for U_{23}^{DCR} rotation scheme.

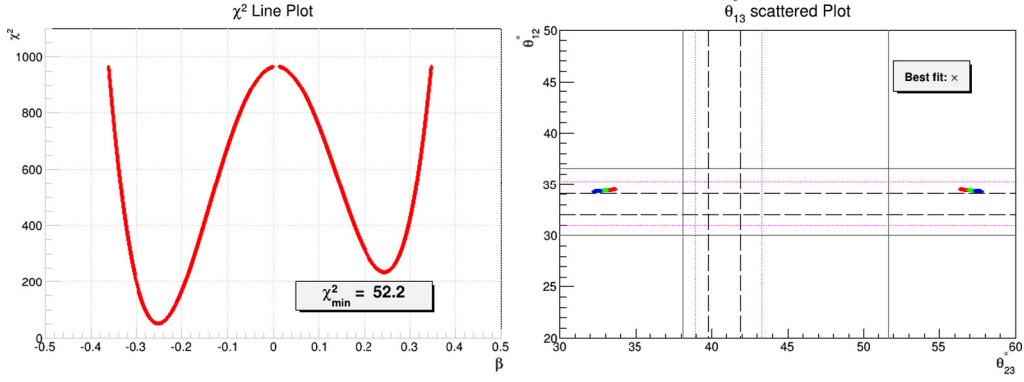

Fig. 14. Line plot of χ^2 (left fig.) vs β (in radians) and scattered plot of θ_{13} (right fig.) over $\theta_{23} - \theta_{12}$ (in degrees) plane for U_{23}^{TBMR} rotation scheme.

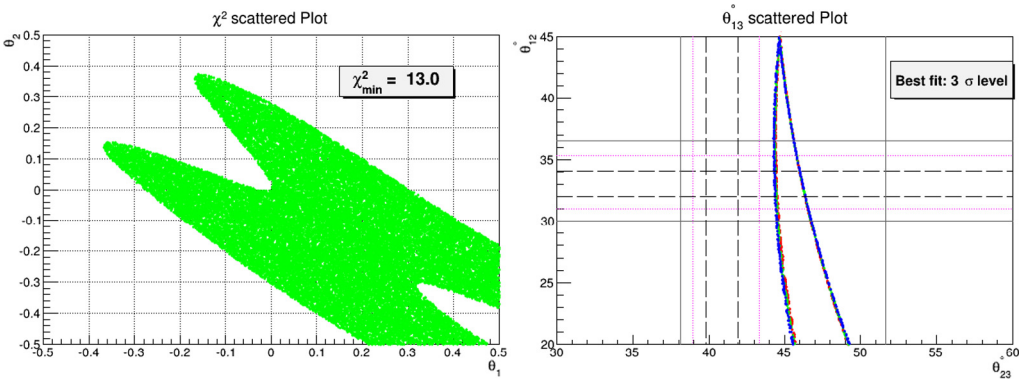

Fig. 15. U^{BML}_{1213} scatter plot of χ^2 (left fig.) over $\alpha - \gamma$ (in radians) plane and θ_{13} (right fig.) over $\theta_{23} - \theta_{12}$ (in degrees) plane. The information about color coding and various horizontal, vertical lines in right fig. is given in text.

(iv) The minimum value of $\chi^2 \sim 151.1$, 162.9 and 52.2 for BM, DC and TBM case respectively.
(v) Thus all cases are ruled out at 3σ level.

6. Rotations-$R^l_{ij}.R^l_{kl}.U$

Here we first consider the perturbations for which modified PMNS matrix is given by $U_{PMNS} = R^l_{ij}.R^l_{kl}.U$. We will investigate the role of these perturbations in fitting the neutrino mixing data.

6.1. 12–13 rotation

This case corresponds to rotations in 12 and 13 sector of these special matrices. Since for small rotation $\sin\theta \approx \theta$ and $\cos\theta \approx 1 - \theta^2$, so the neutrino mixing angles truncated at order O (θ^2) for these rotations are given by

$$\sin\theta_{13} \approx |\alpha U_{23} + \gamma U_{33}|, \tag{6.1}$$

$$\sin\theta_{23} \approx |\frac{(1-\alpha^2)U_{23} - \alpha\gamma U_{33}}{\cos\theta_{13}}|, \tag{6.2}$$

$$\sin\theta_{12} \approx |\frac{U_{12} + \alpha U_{22} + \gamma U_{32} - (\alpha^2+\gamma^2)U_{12}}{\cos\theta_{13}}|. \tag{6.3}$$

Figs. 15–17 show the numerical results corresponding to BM, DC and TBM case with $\theta_1 = \gamma$ and $\theta_2 = \alpha$. The main features of this perturbative matrix are:

(i) From the expression of θ_{23} mixing angle, it is clear that the perturbation parameters enter only at O(θ^2) and thus its value remain close to the original prediction. Thus TBM and BM can become consistent while DC looks off track completely.
(ii) The minimum value of $\chi^2 \sim 13.0$, 173.1 and 13.9 for BM, DC and TBM case respectively.
(iii) In perturbative TBM and BM, its possible to fit all mixing angles at 3σ level while DC case is not consistent. The BM case produces $\theta_{12} \sim 33.30°$, $\theta_{23} \sim 44.41°$ and $\theta_{13} \sim 8.43°$ while TBM gives $\theta_{12} \sim 32.49°$, $\theta_{23} \sim 44.51°$ and $\theta_{13} \sim 8.41°$ for its respective best fit.

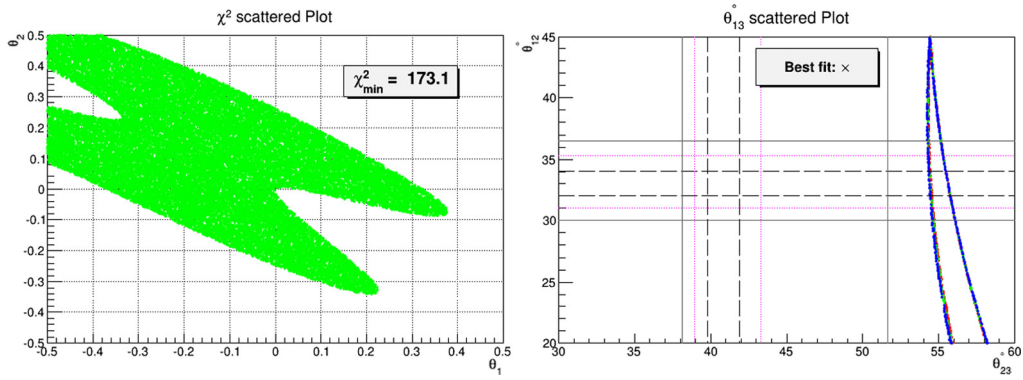

Fig. 16. U_{1213}^{DCL} scatter plot of χ^2 (left fig.) over $\alpha - \gamma$ (in radians) plane and θ_{13} (right fig.) over $\theta_{23} - \theta_{12}$ (in degrees) plane.

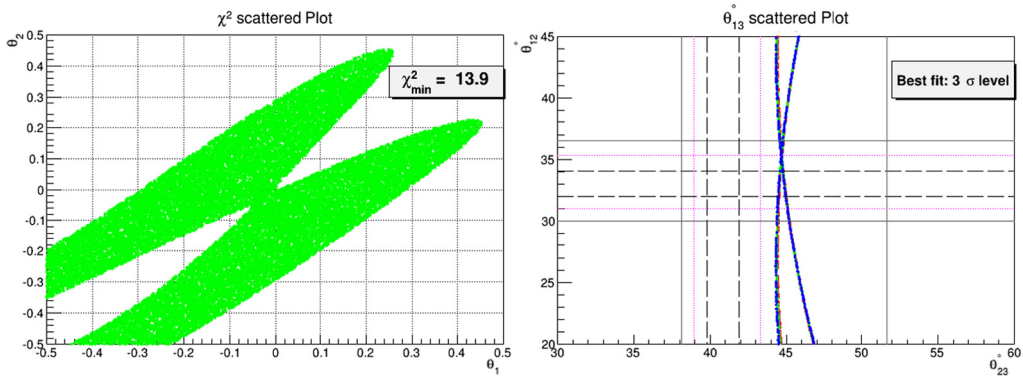

Fig. 17. U_{1213}^{TBML} scatter plot of χ^2 (left fig.) over $\alpha - \gamma$ (in radians) plane and θ_{13} (right fig.) over $\theta_{23} - \theta_{12}$ (in degrees) plane.

6.2. 12–23 rotation

This case corresponds to rotations in 12 and 23 sector of these special matrices. The neutrino mixing angles for small perturbation parameters α and β are given by

$$\sin\theta_{13} \approx |\alpha U_{23} + \alpha\beta U_{33}|, \tag{6.4}$$

$$\sin\theta_{23} \approx |\frac{U_{23} + \beta U_{33} - (\alpha^2 + \beta^2)U_{23}}{\cos\theta_{13}}|, \tag{6.5}$$

$$\sin\theta_{12} \approx |\frac{U_{12} + \alpha U_{22} - \alpha^2 U_{12} + \alpha\beta U_{32}}{\cos\theta_{13}}|. \tag{6.6}$$

Figs. 18–20 corresponds to BM, DC and TBM case respectively with $\theta_1 = \beta$ and $\theta_2 = \alpha$. The main features in this mixing scheme are:

(i) In this scheme, perturbation parameters enters at leading order in all mixing angles and hence show interesting correlations among themselves.

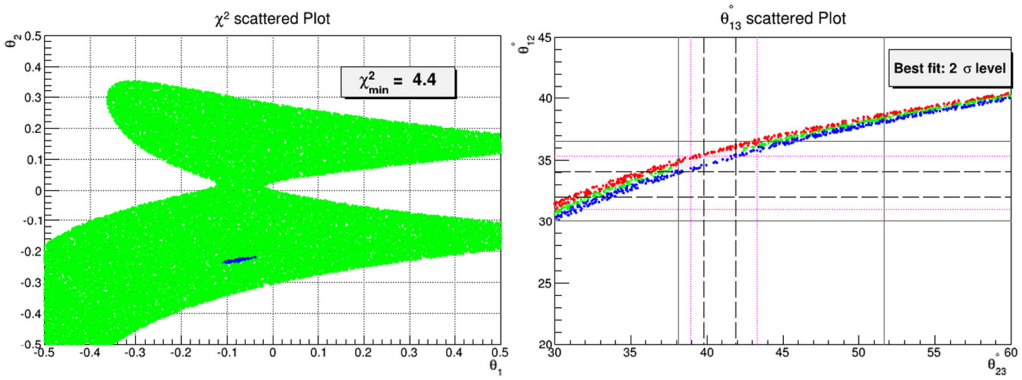

Fig. 18. U_{1223}^{BML} scatter plot of χ^2 (left fig.) over $\alpha - \beta$ (in radians) plane and θ_{13} (right fig.) over $\theta_{23} - \theta_{12}$ (in degrees) plane.

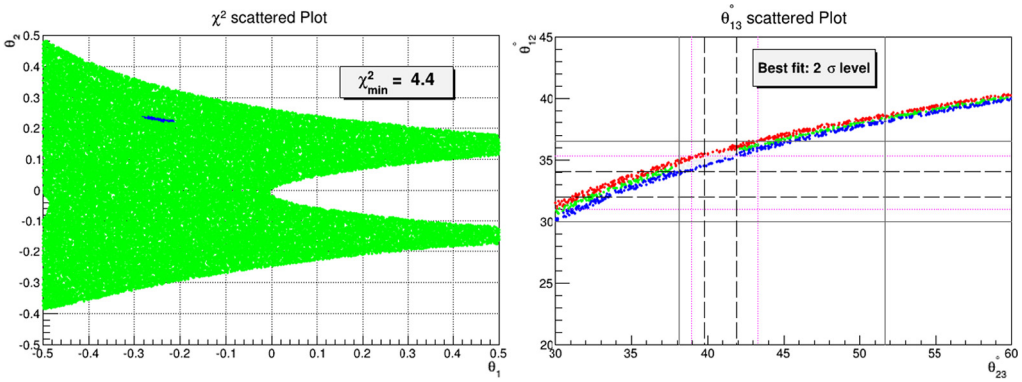

Fig. 19. U_{1223}^{DCL} scatter plot of χ^2 (left fig.) over $\alpha - \beta$ (in radians) plane and θ_{13} (right fig.) over $\theta_{23} - \theta_{12}$ (in degrees) plane.

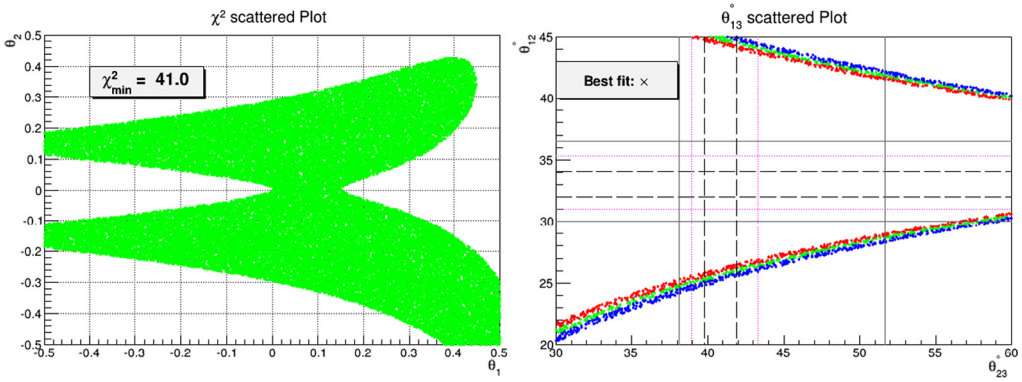

Fig. 20. U_{1223}^{TBML} scatter plot of χ^2 (left fig.) over $\alpha - \beta$ (in radians) plane and θ_{13} (right fig.) over $\theta_{23} - \theta_{12}$ (in degrees) plane.

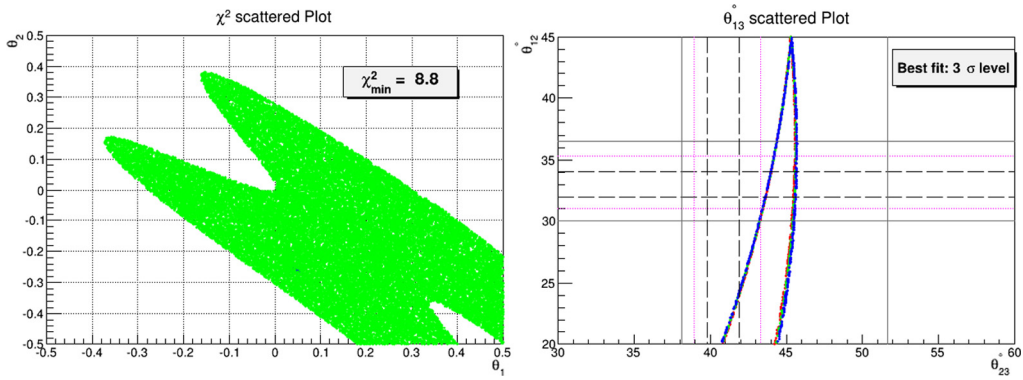

Fig. 21. U_{1312}^{BML} scatter plot of χ^2 (left fig.) over $\gamma - \alpha$ (in radians) plane and θ_{13} (right fig.) over $\theta_{23} - \theta_{12}$ (in degrees) plane.

(ii) It is possible to get $\chi^2 < 5$ for BM and DC case while perturbative TBM is not that promising and corresponding value $\chi^2 > 41$ in parameter space.
(iii) The minimum value of $\chi^2 \sim 4.4$, 4.4 and 41.0 for BM, DC and TBM case respectively.
(iv) In BM and DC case its possible to fit all mixing angles at 2σ level while TBM case is completely excluded at 3σ level. The BM case produces $\theta_{12} \sim 35.03°$, $\theta_{23} \sim 40.04°$ and $\theta_{13} \sim 8.49°$ while DC gives $\theta_{12} \sim 35.07°$, $\theta_{23} \sim 40.05°$ and $\theta_{13} \sim 8.45°$ for its corresponding best fit.

6.3. 13–12 rotation

This case corresponds to rotations in 13 and 12 sector of these special matrices. The neutrino mixing angles for small perturbation parameters α and γ are given by

$$\sin\theta_{13} \approx |\alpha U_{23} + \gamma U_{33}|, \tag{6.7}$$

$$\sin\theta_{23} \approx |\frac{(1-\alpha^2)U_{23}}{\cos\theta_{13}}|, \tag{6.8}$$

$$\sin\theta_{12} \approx |\frac{U_{12} + \alpha U_{22} + \gamma U_{32} - (\alpha^2+\gamma^2)U_{12}}{\cos\theta_{13}}|. \tag{6.9}$$

Figs. 21–23 corresponds to BM, DC and TBM case respectively with $\theta_1 = \gamma$ and $\theta_2 = \alpha$. The main characteristics in this perturbative scheme are given by:

(i) The case is much similar to 12–13 rotation except for θ_{23} where in previous case it got additional $O(\theta^2)$ correction term. Thus for this case also θ_{23} remains close to its unperturbed value.
(ii) The minimum value of $\chi^2 \sim 8.8$, 140.0 and 18.2 for perturbative BM, DC and TBM case respectively.
(iii) For TBM and BM case its possible to fit all mixing angles at 3σ level while DC case is not consistent even at 3σ level. The BM case produces $\theta_{12} \sim 32.38°$, $\theta_{23} \sim 43.69°$ and $\theta_{13} \sim 8.43°$ while TBM gives $\theta_{12} \sim 32.54°$, $\theta_{23} \sim 45.07°$ and $\theta_{13} \sim 8.42°$ for its respective best fit.

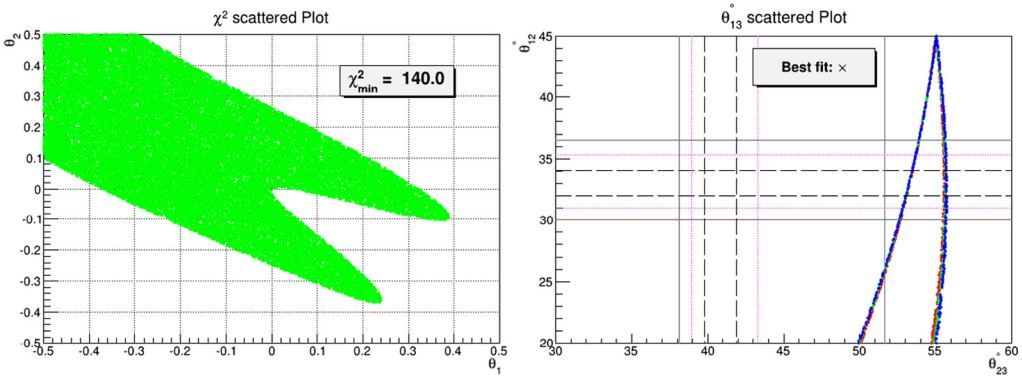

Fig. 22. U_{1312}^{DCL} scatter plot of χ^2 (left fig.) over $\gamma - \alpha$ (in radians) plane and θ_{13} (right fig.) over $\theta_{23} - \theta_{12}$ (in degrees) plane.

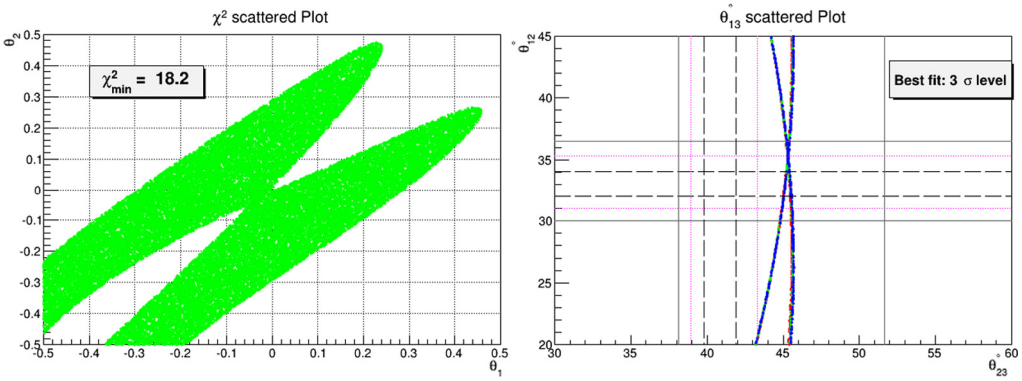

Fig. 23. U_{1312}^{TBML} scatter plot of χ^2 (left fig.) over $\gamma - \alpha$ (in radians) plane and θ_{13} (right fig.) over $\theta_{23} - \theta_{12}$ (in degrees) plane.

6.4. 13–23 rotation

This case corresponds to rotations in 13 and 23 sector of these special matrices. The neutrino mixing angles for small perturbation parameters γ and β are given by

$$\sin\theta_{13} \approx |\gamma U_{33} - \beta\gamma U_{23}|, \tag{6.10}$$

$$\sin\theta_{23} \approx |\frac{U_{23} + \beta U_{33} - \beta^2 U_{23}}{\cos\theta_{13}}|, \tag{6.11}$$

$$\sin\theta_{12} \approx |\frac{U_{12} + \gamma U_{32} - \gamma^2 U_{12} - \beta\gamma U_{22}}{\cos\theta_{13}}|. \tag{6.12}$$

Figs. 24–26 corresponds to BM, DC and TBM case respectively with $\theta_1 = \gamma$ and $\theta_2 = \beta$. The following features define this perturbation scheme:

(i) The parameters β and γ enters into all mixing angles at leading order and thus show good correlations among themselves.
(ii) The minimum value of $\chi^2 \sim 21.0$, 21.0 and 19.7 for BM, DC and TBM case respectively.

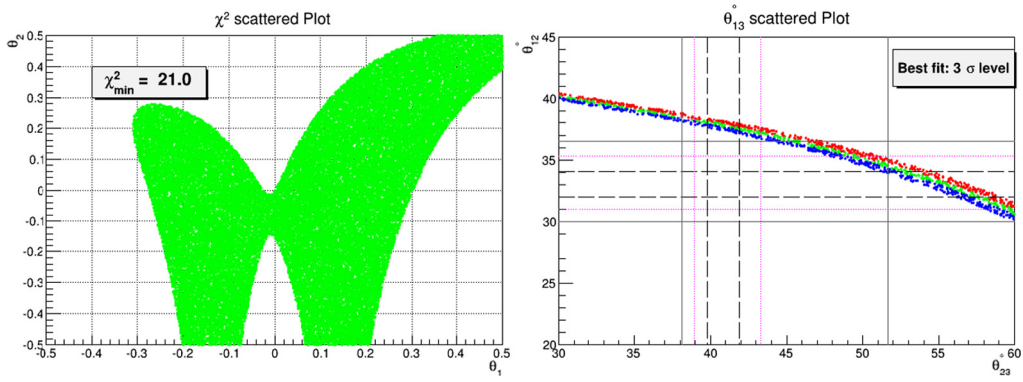

Fig. 24. U_{1323}^{BML} scatter plot of χ^2 (left fig.) over $\gamma - \beta$ (in radians) plane and θ_{13} (right fig.) over $\theta_{23} - \theta_{12}$ (in degrees) plane.

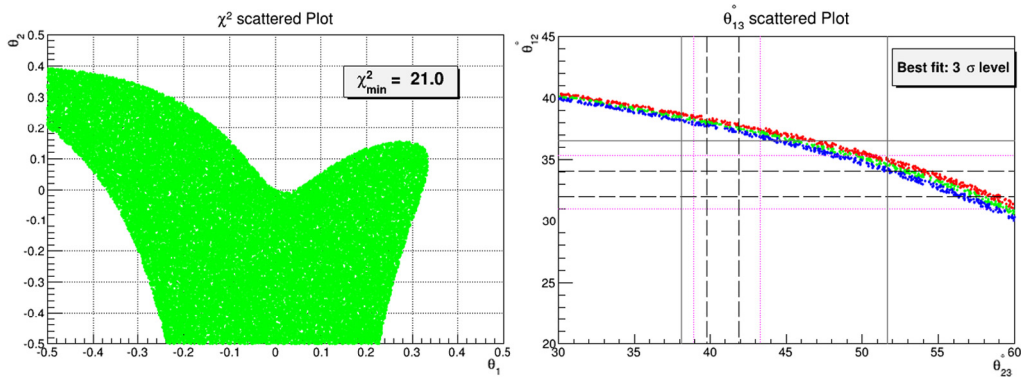

Fig. 25. U_{1323}^{DCL} scatter plot of χ^2 (left fig.) over $\gamma - \beta$ (in radians) plane and θ_{13} (right fig.) over $\theta_{23} - \theta_{12}$ (in degrees) plane.

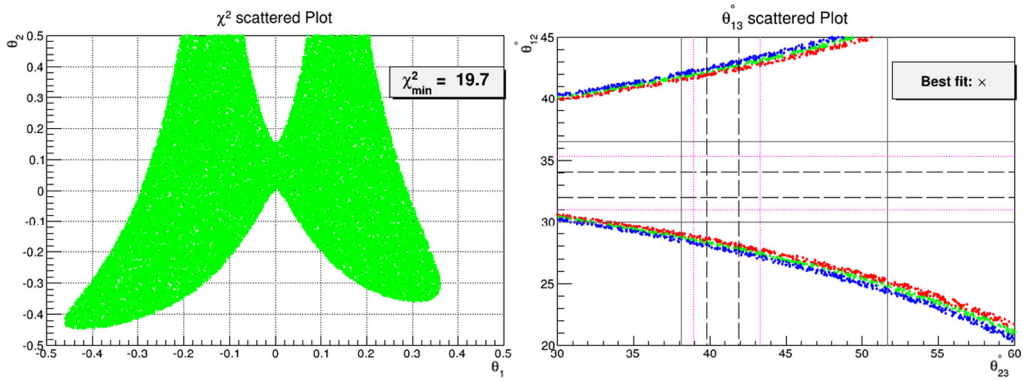

Fig. 26. U_{1323}^{TBML} scatter plot of χ^2 (left fig.) over $\gamma - \beta$ (in radians) plane and θ_{13} (right fig.) over $\theta_{23} - \theta_{12}$ (in degrees) plane.

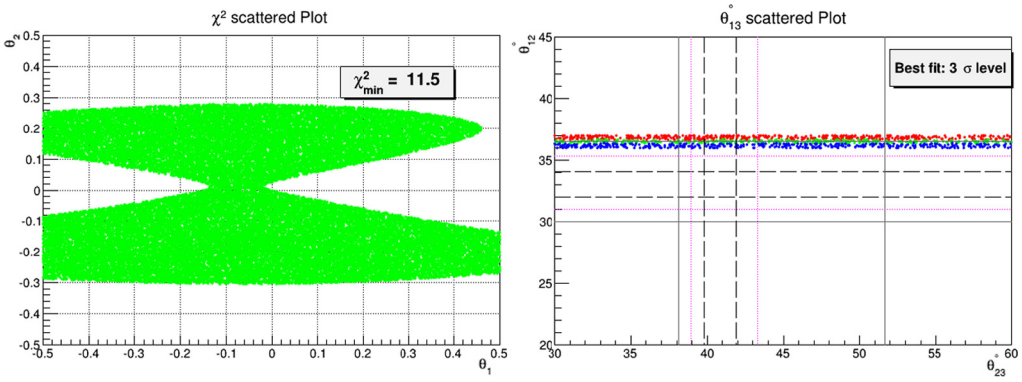

Fig. 27. U^{BML}_{2312} scatter plot of χ^2 (left fig.) over $\beta - \alpha$ (in radians) plane and θ_{13} (right fig.) over $\theta_{23} - \theta_{12}$ (in degrees) plane.

(iii) For this perturbative scheme, TBM is excluded while BM and DC is only consistent at 3σ level.

(iv) The best fit case (i.e. having lowest χ^2) of BM and DC accurately fit θ_{23} and θ_{13} (close to their central values) but it is unable to fit θ_{12} although the achieved value lies quite close to its 3σ boundary. However all angles can be fitted within 3σ range for $\chi^2 = 31.14$ and $\chi^2 = 30.41$ for BM and DC case respectively. The perturbed BM produces $\theta_{12} \sim 36.46°$, $\theta_{23} \sim 45.02°$ and $\theta_{13} \sim 8.62°$ while DC gives $\theta_{12} \sim 36.50°$, $\theta_{23} \sim 44.58°$ and $\theta_{13} \sim 8.71°$ for the mentioned fits. We can observe here that although these fits are at 3σ level but fitted values are quite away from their central values and thus have corresponding $\chi^2 > \chi^2_{min}$.

6.5. 23–12 rotation

This case corresponds to rotations in 23 and 12 sector of these special matrices.

$$\sin\theta_{13} \approx |\alpha U_{23}|, \tag{6.13}$$

$$\sin\theta_{23} \approx |\frac{U_{23} + \beta U_{33} - (\alpha^2 + \beta^2)U_{23}}{\cos\theta_{13}}|, \tag{6.14}$$

$$\sin\theta_{12} \approx |\frac{U_{12} + \alpha U_{22} - \alpha^2 U_{12}}{\cos\theta_{13}}|. \tag{6.15}$$

Figs. 27–29 corresponds to BM, DC and TBM case respectively with $\theta_1 = \beta$ and $\theta_2 = \alpha$. The following are the main characteristics of this perturbative scheme:

(i) The corrections to mixing angle θ_{13} and θ_{12} is only governed by perturbation parameter α. Thus magnitude of parameter α is tightly constrained from fitting of θ_{13}. This in turn permits very narrow ranges for θ_{12} corresponding to negative and positive values of α in parameter space. However θ_{23} mainly depends on β and thus can have wide range of values in parameter space.

(ii) The minimum value of $\chi^2 \sim 11.5$, 35.4 and 32.3 for BM, DC and TBM case respectively.

(iii) The case of TBM and DC is completely excluded while BM is still viable at 3σ level. The perturbed BM produces $\theta_{12} \sim 36.38°$, $\theta_{23} \sim 40.89°$ and $\theta_{13} \sim 8.51°$ for its best fit.

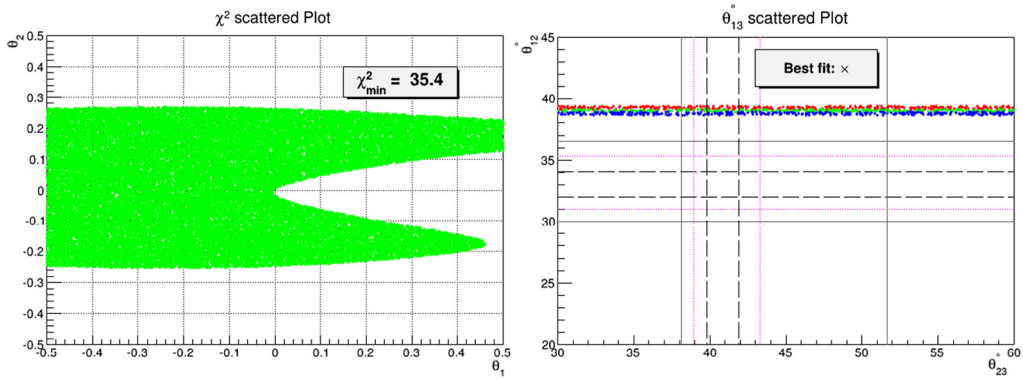

Fig. 28. U_{2312}^{DCL} scatter plot of χ^2 (left fig.) over $\beta - \alpha$ (in radians) plane and θ_{13} (right fig.) over $\theta_{23} - \theta_{12}$ (in degrees) plane.

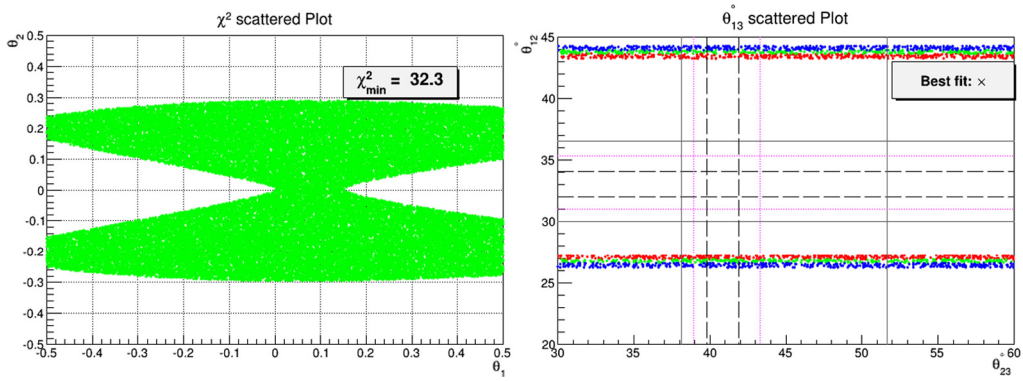

Fig. 29. U_{2312}^{TBML} scatter plot of χ^2 (left fig.) over $\beta - \alpha$ (in radians) plane and θ_{13} (right fig.) over $\theta_{23} - \theta_{12}$ (in degrees) plane.

6.6. 23–13 rotation

For this perturbative scheme, the neutrino mixing angles for small correction parameters β and γ are given by

$$\sin\theta_{13} \approx |\gamma U_{33}|, \tag{6.16}$$

$$\sin\theta_{23} \approx |\frac{U_{23} + \beta U_{33} - \beta^2 U_{23}}{\cos\theta_{13}}|, \tag{6.17}$$

$$\sin\theta_{12} \approx |\frac{U_{12} + \gamma U_{32} - \gamma^2 U_{12}}{\cos\theta_{13}}|. \tag{6.18}$$

Figs. 30–32 corresponds to BM, DC and TBM case respectively with $\theta_1 = \gamma$ and $\theta_2 = \beta$. The main characteristics of this scheme are:

(i) The modifications to mixing angle θ_{13} and θ_{12} is only governed by perturbation parameter γ. Thus magnitude of parameter γ is tightly constrained from fitting of θ_{13}. This in turn allows very narrow ranges for θ_{12} corresponding to negative and positive values of γ in parameter

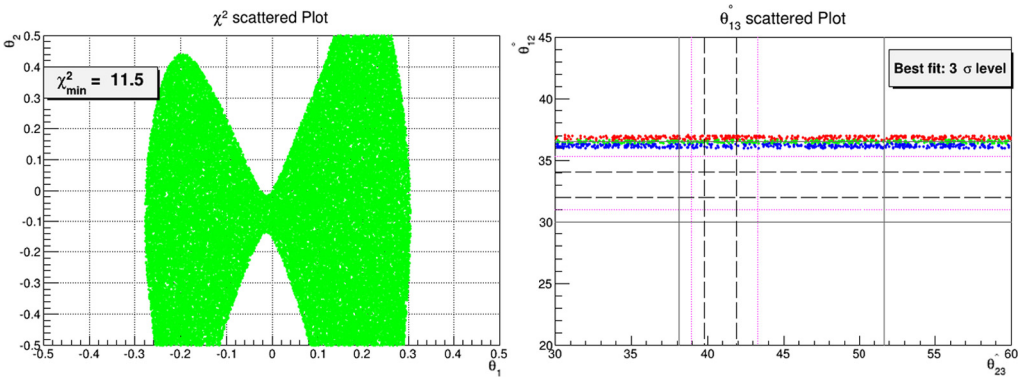

Fig. 30. U_{2313}^{BML} scatter plot of χ^2 (left fig.) over $\beta - \gamma$ (in radians) plane and θ_{13} (right fig.) over $\theta_{23} - \theta_{12}$ (in degrees) plane.

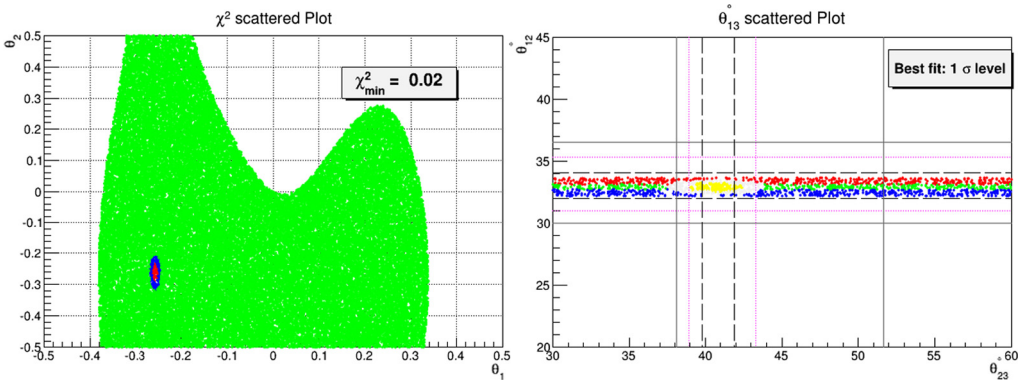

Fig. 31. U_{2313}^{DCL} scatter plot of χ^2 (left fig.) over $\beta - \gamma$ (in radians) plane and θ_{13} (right fig.) over $\theta_{23} - \theta_{12}$ (in degrees) plane.

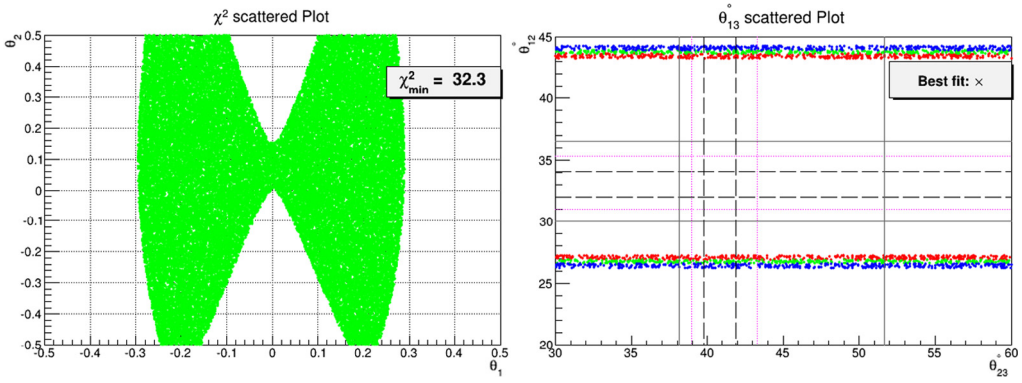

Fig. 32. U_{2313}^{TBML} scatter plot of χ^2 (left fig.) over $\beta - \gamma$ (in radians) plane and θ_{13} (right fig.) over $\theta_{23} - \theta_{12}$ (in degrees) plane.

space. However θ_{23} solely depends on β and thus can have wide range of possible values in parameter space.

(ii) For this rotation scheme its possible to get $\chi^2 < 1$ for DC in tiny viable parameter space while for BM and TBM cases $\chi^2 > 11$ and $\chi^2 > 32$ respectively.

(iii) The minimum value of $\chi^2 \sim 11.5$, 0.02 and 32.3 for BM, DC and TBM case respectively.

(iv) The TBM case is completely excluded as it prefers much lower value of θ_{12} while BM can only be consistent at 3σ level. Here DC case is most preferable as it can fit all mixing angles within 1σ range. The BM case produces $\theta_{12} \sim 36.42°$, $\theta_{23} \sim 40.96°$ and $\theta_{13} \sim 8.48°$ while DC gives $\theta_{12} \sim 32.90°$, $\theta_{23} \sim 40.77°$ and $\theta_{13} \sim 8.42°$ for its respective best fit.

7. Rotations-$U.R^r_{ij}.R^r_{kl}$

Now we comes to the perturbations for which modified PMNS matrix is given by $U_{PMNS} = U.R^r_{ij}.R^r_{kl}$. We will investigate the role of these corrections in fitting the neutrino mixing data.

7.1. 12–13 rotation

This case corresponds to rotations in 12 and 13 sector of these special matrices. The neutrino mixing angles truncated at order O (θ^2) for this mixing scheme is given by

$$\sin\theta_{13} \approx |-\gamma U_{11} + \alpha\gamma U_{12}|, \tag{7.1}$$

$$\sin\theta_{23} \approx |\frac{U_{23} + \gamma U_{21} - \gamma^2 U_{23} - \alpha\gamma U_{22}}{\cos\theta_{13}}|, \tag{7.2}$$

$$\sin\theta_{12} \approx |\frac{U_{12} + \alpha U_{11} - \alpha^2 U_{12}}{\cos\theta_{13}}|. \tag{7.3}$$

In Figs. 33–35, we present the numerical results corresponding to BM, DC and TBM case. The main features of this perturbative scheme with $\theta_1 = \gamma$ and $\theta_2 = \alpha$ are given by:

(i) The perturbation parameters (α, γ) enters into these mixing angles at leading order and thus exhibit good correlations among themselves.

(ii) Here parameter space prefers two regions for mixing angles. In TBM and BM case for first allowed region $\theta_{23} \sim 40°$ while for 2nd it lies around 50°. In DC case higher θ_{23} region remains outside 3σ band while lower θ_{23} remains around 50°.

(iii) The minimum value of $\chi^2 \sim 1.1$, 65.8 and 1.7 for BM, DC and TBM case respectively.

(iv) It is possible to fit all mixing angles at 1σ level for TBM and BM while DC case can only be consistent at 3σ level. The DC case produces $\theta_{12} \sim 34.61°$, $\theta_{23} \sim 48.92°$ and $\theta_{13} \sim 8.48°$ for its best fit.

(v) The best fit case (with lowest χ^2) of BM and TBM very accurately fit θ_{12} and θ_{13} (close to their central values) but it keeps θ_{23} in its 2σ range quite close to its 1σ boundary. However all angles can be fitted within 1σ range for $\chi^2 = 2.15$ and $\chi^2 = 2.05$ for BM and TBM case respectively. The perturbed BM produces $\theta_{12} \sim 32.05°$, $\theta_{23} \sim 39.82°$ and $\theta_{13} \sim 8.32°$ while TBM gives $\theta_{12} \sim 32.03°$, $\theta_{23} \sim 39.81°$ and $\theta_{13} \sim 8.33°$ for the mentioned fits. Although these fits are at 1σ level but fitted values of mixing angles are away from their central values and thus have corresponding $\chi^2 > \chi^2_{min}$.

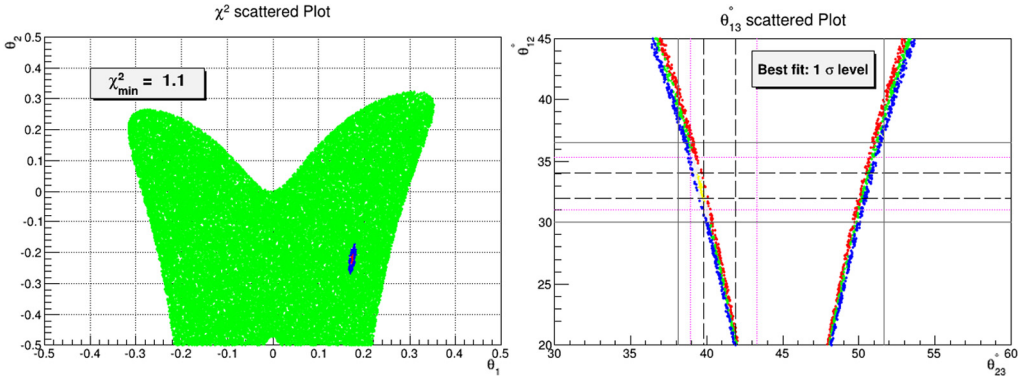

Fig. 33. U_{1213}^{BMR} scatter plot of χ^2 (left fig.) over $\alpha - \gamma$ (in radians) plane and θ_{13} (right fig.) over $\theta_{23} - \theta_{12}$ (in degrees) plane.

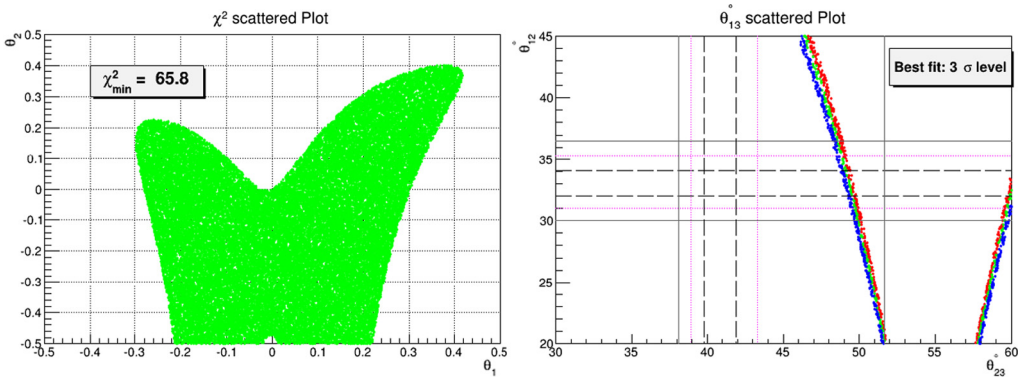

Fig. 34. U_{1213}^{DCR} scatter plot of χ^2 (left fig.) over $\alpha - \gamma$ (in radians) plane and θ_{13} (right fig.) over $\theta_{23} - \theta_{12}$ (in degrees) plane.

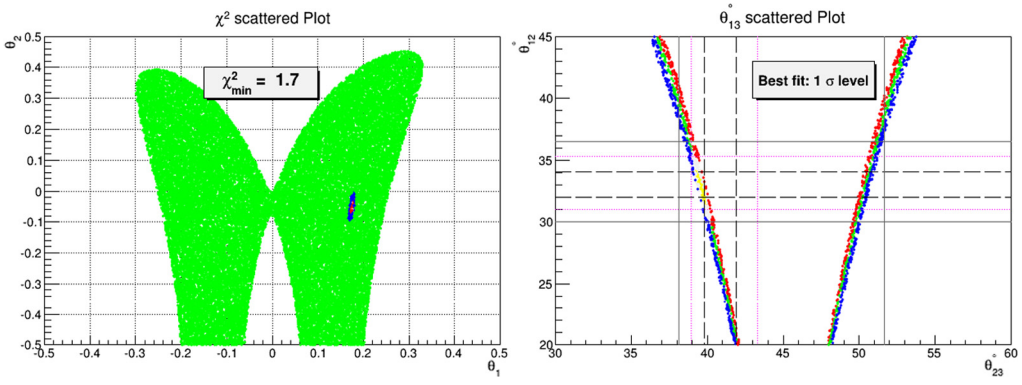

Fig. 35. U_{1213}^{TBMR} scatter plot of χ^2 (left fig.) over $\alpha - \gamma$ (in radians) plane and θ_{13} (right fig.) over $\theta_{23} - \theta_{12}$ (in degrees) plane.

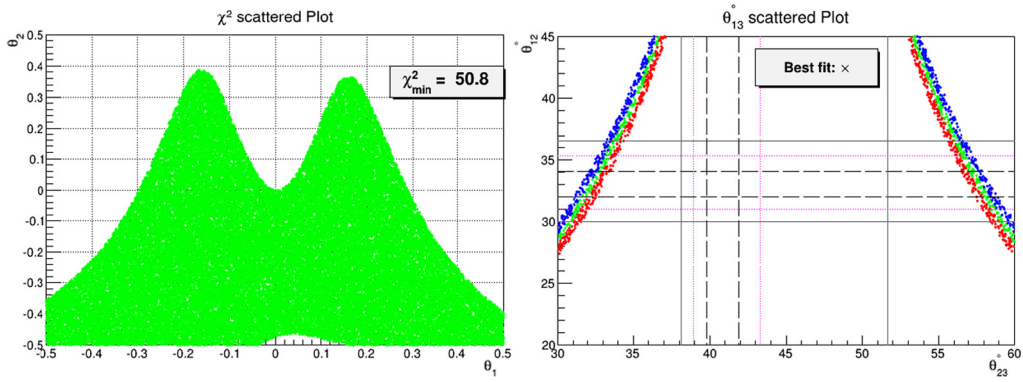

Fig. 36. U_{1223}^{BMR} scatter plot of χ^2 (left fig.) over $\alpha - \beta$ (in radians) plane and θ_{13} (right fig.) over $\theta_{23} - \theta_{12}$ (in degrees) plane.

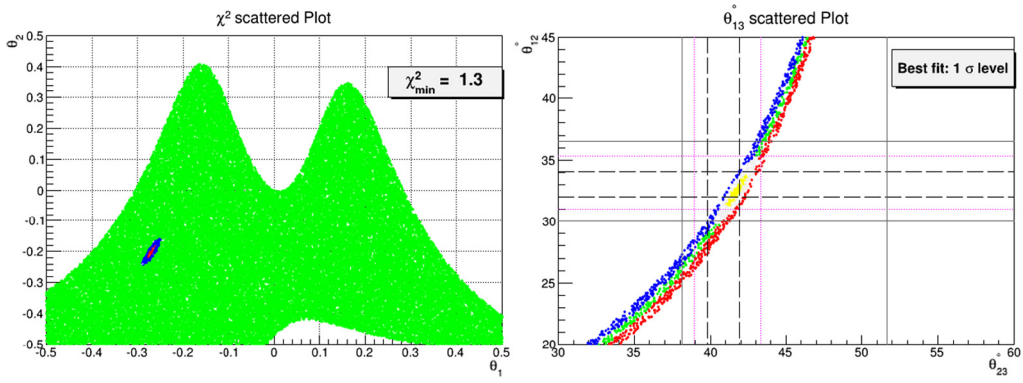

Fig. 37. U_{1223}^{DCR} scatter plot of χ^2 (left fig.) over $\alpha - \beta$ (in radians) plane and θ_{13} (right fig.) over $\theta_{23} - \theta_{12}$ (in degrees) plane.

7.2. 12–23 rotation

This case corresponds to rotations in 12 and 23 sector of these special matrices. The neutrino mixing angles for small perturbation parameters α and β are given by

$$\sin\theta_{13} \approx |\beta U_{12} + \alpha\beta U_{11}|, \tag{7.4}$$

$$\sin\theta_{23} \approx |\frac{U_{23} + \beta U_{22} - \beta^2 U_{23} + \alpha\beta U_{21}}{\cos\theta_{13}}|, \tag{7.5}$$

$$\sin\theta_{12} \approx |\frac{U_{12} + \alpha U_{11} - (\alpha^2 + \beta^2) U_{12}}{\cos\theta_{13}}|. \tag{7.6}$$

Figs. 36–38 corresponds to BM, DC and TBM case respectively with $\theta_1 = \beta$ and $\theta_2 = \alpha$. The main outlines of this scheme are given as:

(i) The perturbation parameters enters at leading order into these mixing angles and hence show interesting correlations among themselves.

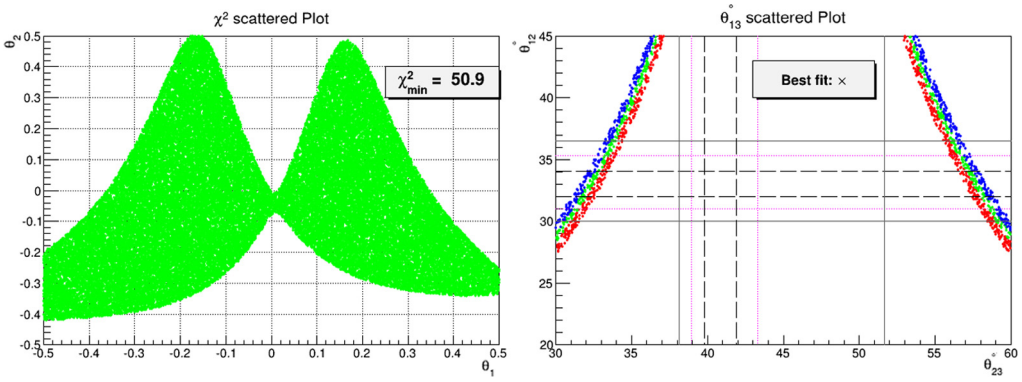

Fig. 38. U_{1223}^{TBMR} scatter plot of χ^2 (left fig.) over $\alpha - \beta$ (in radians) plane and θ_{13} (right fig.) over $\theta_{23} - \theta_{12}$ (in degrees) plane.

(ii) This case is unfavorable for TBM and BM as $\chi^2 > 50$ in all parameter space. However for DC case it is possible to get $\chi^2 < 2$ in a tiny parameter region.
(iii) The minimum value of $\chi^2 \sim 50.8$, 1.3 and 50.9 for BM, DC and TBM case respectively.
(iv) TBM and BM is completely excluded while DC case can fit mixing angles at 1σ level. The perturbative DC produces $\theta_{12} \sim 32.57°$, $\theta_{23} \sim 41.78°$ and $\theta_{13} \sim 8.44°$ for its respective best fit.

7.3. 13–12 rotation

This case corresponds to rotations in 13 and 12 sector of these special matrices. The neutrino mixing angles for small perturbation parameters α and γ are given by

$$\sin\theta_{13} \approx |\gamma U_{11}|, \tag{7.7}$$

$$\sin\theta_{23} \approx \left|\frac{U_{23} + \gamma U_{21} - \gamma^2 U_{23}}{\cos\theta_{13}}\right|, \tag{7.8}$$

$$\sin\theta_{12} \approx \left|\frac{U_{12} + \alpha U_{11} - \alpha^2 U_{12}}{\cos\theta_{13}}\right|. \tag{7.9}$$

Figs. 39–41 corresponds to BM, DC and TBM case respectively with $\theta_1 = \gamma$ and $\theta_2 = \alpha$.

(i) The corrections to mixing angle θ_{13} and θ_{23} is only governed by perturbation parameter γ. Thus magnitude of parameter γ is tightly constrained from fitting of θ_{13}. This in turn permits very narrow ranges for θ_{23} corresponding to negative and positive values of γ in parameter space. However θ_{12} solely depends on α and thus can have wide range of possible values in parameter space.
(ii) The minimum value of $\chi^2 \sim 15.5$, 28.0 and 2.6 for BM, DC and TBM case respectively.
(iii) DC and TBM are consistent at 3σ and 2σ level while BM is not consistent even at 3σ level. The DC case produces $\theta_{12} \sim 32.89°$, $\theta_{23} \sim 46.11°$ and $\theta_{13} \sim 8.52°$ while TBM gives $\theta_{12} \sim 32.98°$, $\theta_{23} \sim 39.0°$ and $\theta_{13} \sim 8.40°$ for its respective best fit.

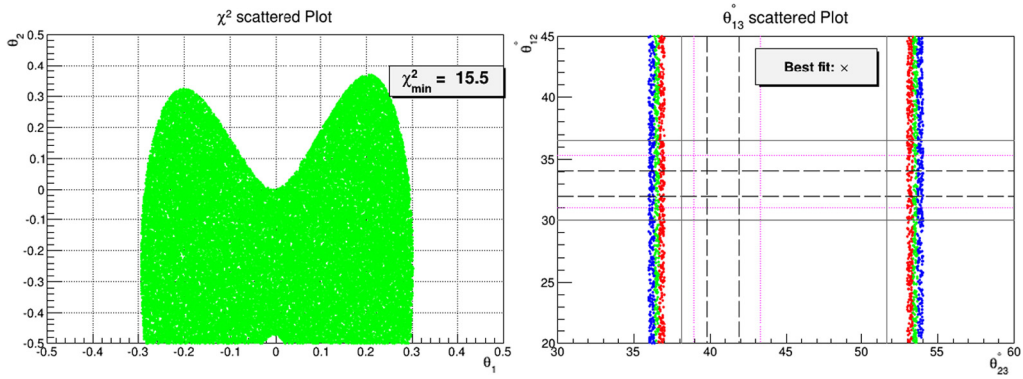

Fig. 39. U_{1312}^{BMR} scatter plot of χ^2 (left fig.) over $\gamma - \alpha$ (in radians) plane and θ_{13} (right fig.) over $\theta_{23} - \theta_{12}$ (in degrees) plane.

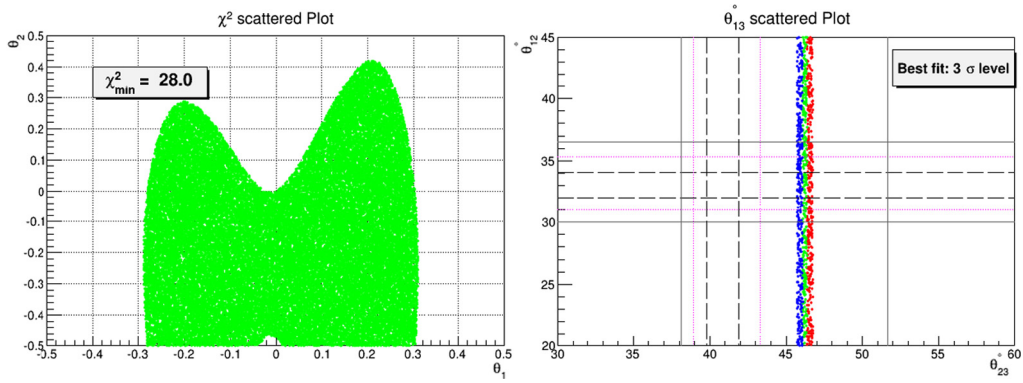

Fig. 40. U_{1312}^{DCR} scatter plot of χ^2 (left fig.) over $\gamma - \alpha$ (in radians) plane and θ_{13} (right fig.) over $\theta_{23} - \theta_{12}$ (in degrees) plane.

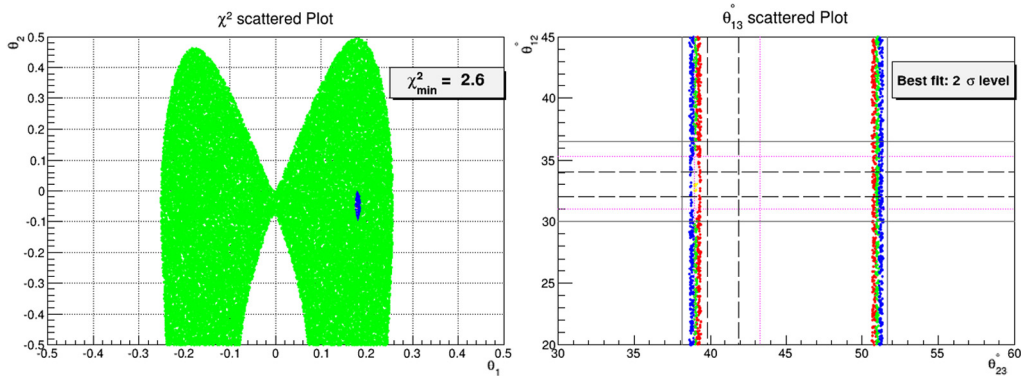

Fig. 41. U_{1312}^{TBMR} scatter plot of χ^2 (left fig.) over $\gamma - \alpha$ (in radians) plane and θ_{13} (right fig.) over $\theta_{23} - \theta_{12}$ (in degrees) plane.

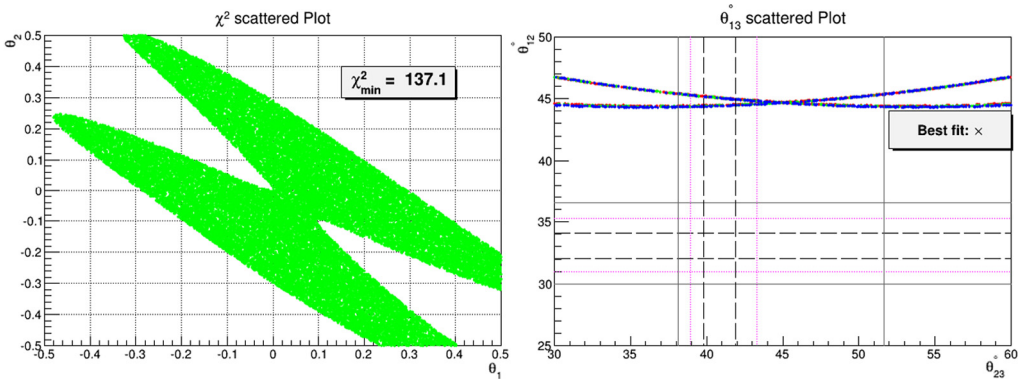

Fig. 42. U_{1323}^{BMR} scatter plot of χ^2 (left fig.) over $\gamma - \beta$ (in radians) plane and θ_{13} (right fig.) over $\theta_{23} - \theta_{12}$ (in degrees) plane.

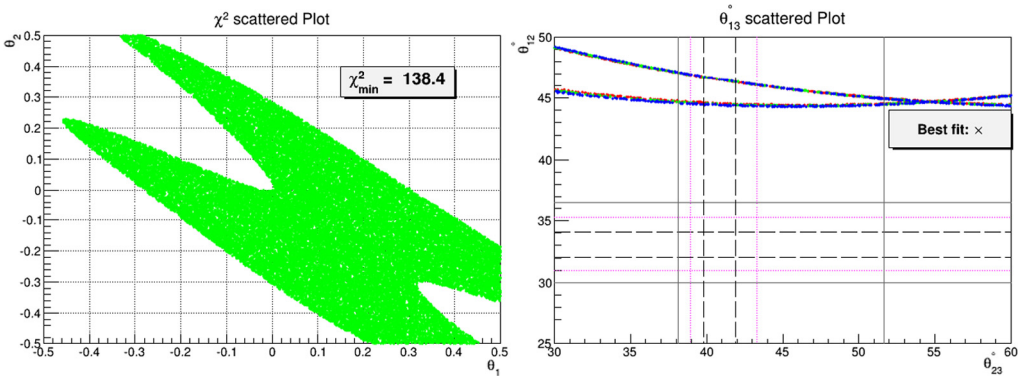

Fig. 43. U_{1323}^{DCR} scatter plot of χ^2 (left fig.) over $\gamma - \beta$ (in radians) plane and θ_{13} (right fig.) over $\theta_{23} - \theta_{12}$ (in degrees) plane.

7.4. 13–23 rotation

This case corresponds to rotations in 13 and 23 sector of these special matrices. The neutrino mixing angles for small perturbation parameters γ and β are given by

$$\sin\theta_{13} \approx |\beta U_{12} + \gamma U_{11}|, \tag{7.10}$$

$$\sin\theta_{23} \approx |\frac{U_{23} + \beta U_{22} + \gamma U_{21} - (\beta^2 + \gamma^2)U_{23}}{\cos\theta_{13}}|, \tag{7.11}$$

$$\sin\theta_{12} \approx |\frac{(1-\beta^2)U_{12} - \beta\gamma U_{11}}{\cos\theta_{13}}|. \tag{7.12}$$

Figs. 42–44 corresponds to BM, DC and TBM case respectively with $\theta_1 = \gamma$ and $\theta_2 = \beta$.

(i) For this rotation scheme, θ_{12} receives corrections only at $O(\theta^2)$ and thus its value remain close to its unperturbed value.

(ii) The minimum value of $\chi^2 \sim 137.1$, 138.4 and 3.0 for BM, DC and TBM case respectively.

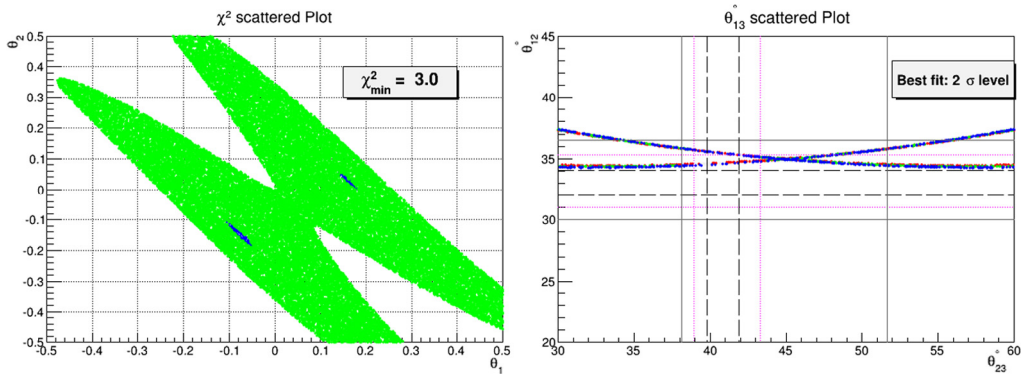

Fig. 44. U_{1323}^{TBMR} scatter plot of χ^2 (left fig.) over $\gamma - \beta$ (in radians) plane and θ_{13} (right fig.) over $\theta_{23} - \theta_{12}$ (in degrees) plane.

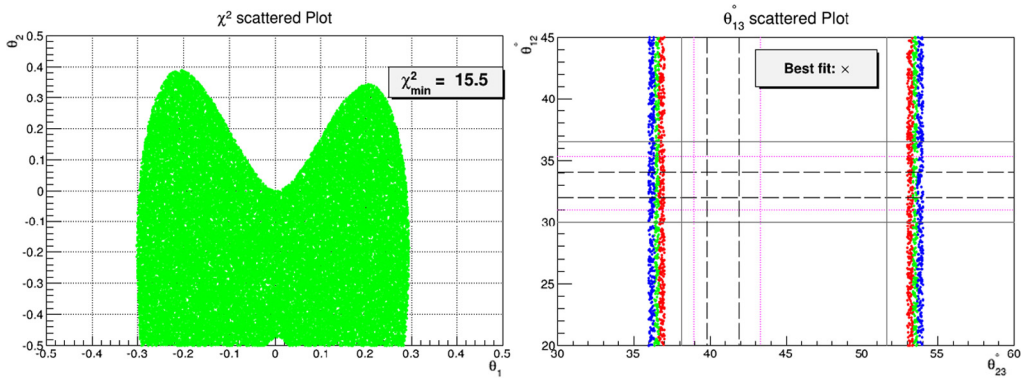

Fig. 45. U_{2312}^{BMR} scatter plot of χ^2 (left fig.) over $\beta - \alpha$ (in radians) plane and θ_{13} (right fig.) over $\theta_{23} - \theta_{12}$ (in degrees) plane.

(iii) All mixing angles can be fitted at 2σ level in TBM while BM and DC case is excluded as their unperturbed θ_{12} value is quite away from 3σ boundary. The perturbative TBM produces $\theta_{12} \sim 34.66°$, $\theta_{23} \sim 41.34°$ and $\theta_{13} \sim 8.41°$ for its best fit.

7.5. 23–12 rotation

This case corresponds to rotations in 23 and 12 sector of these special matrices.

$$\sin\theta_{13} \approx |\beta U_{12}|, \tag{7.13}$$

$$\sin\theta_{23} \approx |\frac{U_{23} + \beta U_{22} - \beta^2 U_{23}}{\cos\theta_{13}}|, \tag{7.14}$$

$$\sin\theta_{12} \approx |\frac{U_{12} + \alpha U_{11} - (\alpha^2 + \beta^2) U_{12}}{\cos\theta_{13}}|. \tag{7.15}$$

Figs. 45–47 corresponds to BM, DC and TBM case respectively with $\theta_1 = \beta$ and $\theta_2 = \alpha$.

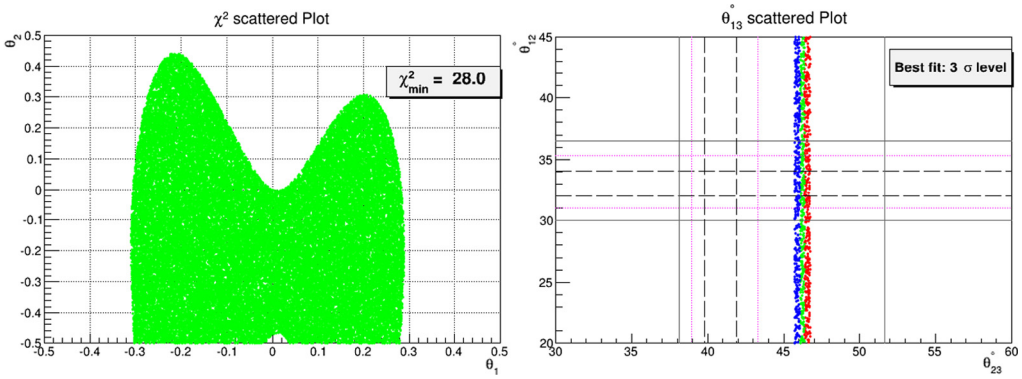

Fig. 46. U_{2312}^{DCR} scatter plot of χ^2 (left fig.) over $\beta - \alpha$ (in radians) plane and θ_{13} (right fig.) over $\theta_{23} - \theta_{12}$ (in degrees) plane.

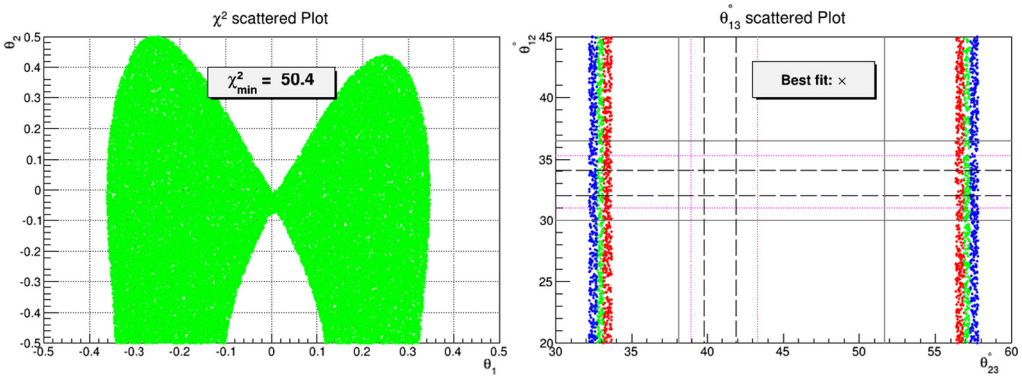

Fig. 47. U_{2312}^{TBMR} scatter plot of χ^2 (left fig.) over $\beta - \alpha$ (in radians) plane and θ_{13} (right fig.) over $\theta_{23} - \theta_{12}$ (in degrees) plane.

(i) The corrections to mixing angle θ_{13} and θ_{23} is only governed by perturbation parameter β. Thus magnitude of parameter β is tightly constrained from fitting of θ_{13}. This in turn allows only very narrow ranges for θ_{23} corresponding to negative and positive values of β in parameter space. However θ_{12} solely depends on α and thus can have wide range of possible values in parameter space.

(ii) The minimum value of $\chi^2 \sim 15.5$, 28.0 and 50.4 for BM, DC and TBM case respectively.

(iii) BM and TBM case is completely excluded while DC is allowed at 3σ level. The perturbative DC case produces $\theta_{12} \sim 32.95°$, $\theta_{23} \sim 46.09°$ and $\theta_{13} \sim 8.54°$ for its respective best fit.

7.6. 23–13 rotation

This case is much similar to 13–12 rotation with interchange of expressions for θ_{12} and θ_{23} mixing angles. The neutrino mixing angles for small perturbation parameters β and γ are given by

$$\sin\theta_{13} \approx |\beta U_{12} + \gamma U_{11}|, \tag{7.16}$$

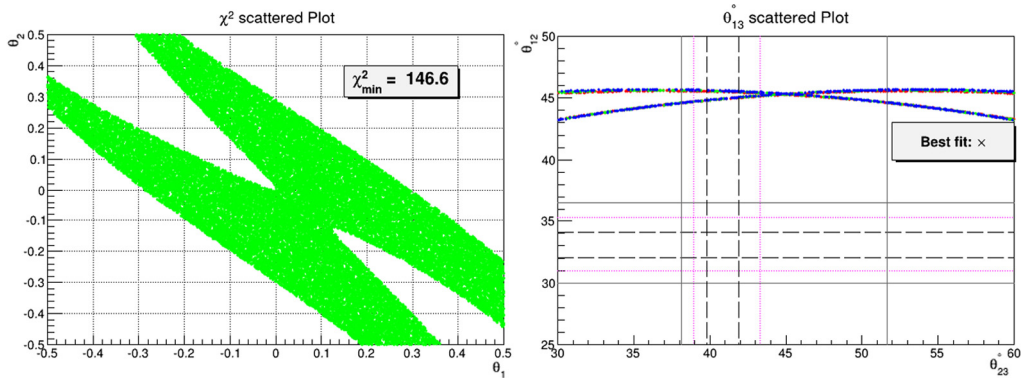

Fig. 48. U_{2313}^{BMR} scatter plot of χ^2 (left fig.) over $\beta - \gamma$ (in radians) plane and θ_{13} (right fig.) over $\theta_{23} - \theta_{12}$ (in degrees) plane.

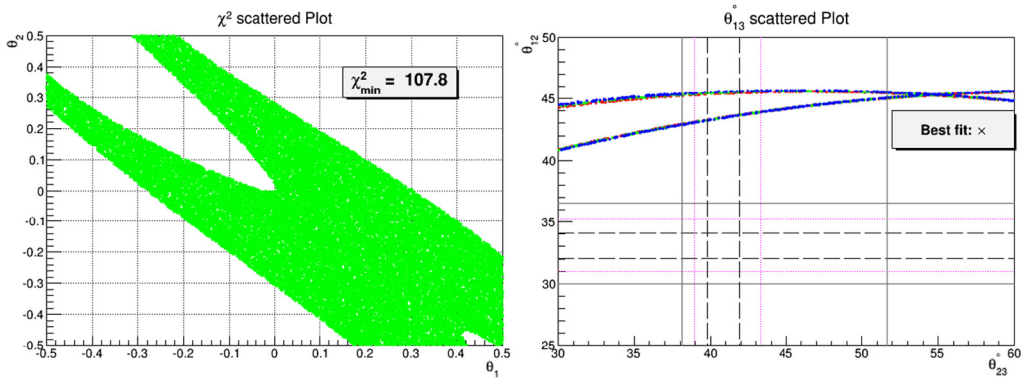

Fig. 49. U_{2313}^{DCR} scatter plot of χ^2 (left fig.) over $\beta - \gamma$ (in radians) plane and θ_{13} (right fig.) over $\theta_{23} - \theta_{12}$ (in degrees) plane.

$$\sin\theta_{23} \approx |\frac{U_{23} + \beta U_{22} + \gamma U_{21} - (\beta^2 + \gamma^2)U_{23}}{\cos\theta_{13}}|, \tag{7.17}$$

$$\sin\theta_{12} \approx |\frac{(\beta^2 - 1)U_{12}}{\cos\theta_{13}}|. \tag{7.18}$$

Figs. 48–50 corresponds to BM, DC and TBM case respectively with $\theta_1 = \gamma$ and $\theta_2 = \beta$. The main characteristic features of this scheme are:

(i) In this rotation scheme, θ_{12} angle receives corrections at $O(\theta^2)$ and thus its value remain close to its unperturbed value.
(ii) The minimum value of $\chi^2 \sim 146.6$, 107.8 and 5.2 for BM, DC and TBM case respectively.
(iii) Thus BM and DC case is completely excluded as $\theta_{12} \sim 45°$ which is well away from 3σ line. However TBM is still consistent at 2σ level. The TBM case produces $\theta_{12} \sim 35.19°$, $\theta_{23} \sim 39.80°$ and $\theta_{13} \sim 8.44°$ for its corresponding best fit.

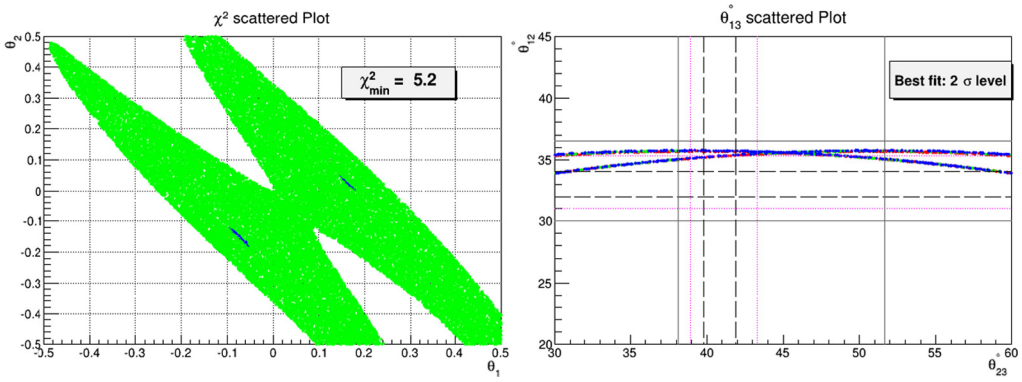

Fig. 50. U_{2313}^{TBMR} scatter plot of χ^2 (left fig.) over $\beta - \gamma$ (in radians) plane and θ_{13} (right fig.) over $\theta_{23} - \theta_{12}$ (in degrees) plane.

8. Summary and conclusions

Tribimaximal (TBM), bimaximal (BM) and Democratic (DC) mixing matrices offers to explain the neutrino mixing data with a common prediction of vanishing reactor mixing angle. The atmospheric mixing angle (θ_{23}) is maximal in TBM and BM scenarios while it takes the larger value of 54.7° for DC mixing. The value of solar mixing angle (θ_{12}) is maximal in BM and DC scenarios while its value is 35.3° for TBM case. However experimental observation of non zero reactor mixing angle ($\theta_{13} \approx 8°$) and departure of other two mixing angles from maximality is asking for corrections in these mixing schemes.

In this study, we investigated the perturbations around TBM, BM and DC mixing scenarios. These modifications are expressed in terms of three orthogonal rotation matrices R_{12}, R_{13} and R_{23} which acts on 12, 13 and 23 sector of unperturbed PMNS matrix respectively. We looked into various possible cases that are governed by one and two rotation matrices with corresponding modified PMNS matrices of the forms $\left(R_{ij} \cdot U,\ R_{ij} \cdot R_{kl} \cdot U,\ U \cdot R_{ij},\ U \cdot R_{ij} \cdot R_{kl}\right)$ where U is any one of these special matrices. As the form of PMNS matrix is given by $U_{PMNS} = U_l^{\dagger} U_\nu$ so these corrections may originate from charged lepton and neutrino sector respectively. In this study, we restricted ourselves to CP conserving case by setting phases to be zero. The effects of CP violation on mixing angles will be reported somewhere else. For our analysis we constructed χ^2 function which is a measure of deviation from experimental best fit values of mixing angles. The numerical findings are presented in terms of χ^2 vs perturbation parameters and as correlations among different neutrino mixing angles. The final results are summarized in Table 4 and Table 5 for single and double rotation cases respectively. For the sake of completion, we also included the results of $R_{ij} \cdot U \cdot R_{kl}$ perturbative scheme [19] and updated them for new mixing data in Table 6.

The rotation $R_{12} \cdot U$, imparts negligible corrections to θ_{23} and thus its value remain close to its unperturbed prediction. Here BM case can achieve $\chi^2 \sim 24$ and thus allowed at 3σ level while other two cases are not consistent. In rotation $R_{13} \cdot U$, θ_{23} receives very minor corrections through θ_{13} and thus stays close to its original prediction. The BM case is consistent at 3σ level while other two cases are not allowed. For $R_{23} \cdot U$ case, θ_{13} is still zero and thus it was not investigated any further. The rotation $U \cdot R_{12}$, doesn't impart corrections to 13 mixing angle and thus we left its further discussion. For $U \cdot R_{13}$, θ_{12} receives very minor corrections

only through θ_{13} and thus its range remains quite close to its unperturbed value. The only perturbed TBM is allowed at 3σ level while other two mixing schemes are not consistent with mixing data. The $U \cdot R_{23}$ rotation scheme is not consistent with mixing data for all three mixing schemes.

For rotation $R_{12} \cdot R_{13} \cdot U$, θ_{23} remain close to its unperturbed value. Thus TBM and BM cases can be consistent at 3σ level while DC is not allowed. The rotation $R_{12} \cdot R_{23} \cdot U$ for BM and DC can fit all mixing angles within 2σ level. However TBM case is completely excluded for this rotation. The perturbation scheme $R_{13} \cdot R_{12} \cdot U$ scheme is much similar to $R_{12} \cdot R_{13} \cdot U$. Here also TBM and BM cases can be consistent at 3σ level while DC is not consistent. For rotation $R_{13} \cdot R_{23} \cdot U$, TBM case is excluded while BM and DC is consistent at 3σ level. In $R_{23} \cdot R_{12} \cdot U$, TBM and DC is completely excluded while BM can only be viable at 3σ level. Thus this case is not much preferable. The perturbation scheme $R_{23} \cdot R_{13} \cdot U$ is much favorable for DC case as it successfully fits all mixing angles at 1σ level with lowest value of χ^2 among all mixing schemes. However TBM case is excluded for this rotation while BM can only be viable at 3σ level.

The perturbation scheme $U \cdot R_{12} \cdot R_{13}$ is much preferable since it is possible to fit all mixing angles within 1σ range for TBM and BM case. However DC case can only be allowed at 3σ level. The rotation scheme $U \cdot R_{12} \cdot R_{23}$ is only preferable for DC while the other two cases in scheme are excluded at 3σ level. The mixing angles can be fitted at 1σ level in this rotation for DC case. In rotation $U \cdot R_{13} \cdot R_{12}$, it is possible to fit all mixing angles within 2σ range for perturbed TBM matrix and 3σ level for perturbed DC case. However BM is not viable as it failed to fit mixing angles even at 3σ level. The perturbed rotation $U \cdot R_{13} \cdot R_{23}$ imparts corrections to θ_{12} only at $O(\theta^2)$. Thus its value remain quite close to its original value and hence BM and DC cases are excluded while TBM can be consistent at 2σ level. The rotation scheme $U \cdot R_{23} \cdot R_{12}$ is only little preferable for DC case as it is possible to fit mixing angles at 3σ level while other two cases are not consistent. Like $U \cdot R_{13} \cdot R_{23}$ case, rotation scheme $U \cdot R_{23} \cdot R_{13}$ also imparts negligible corrections to θ_{12}. Thus BM and DC case is excluded while perturbed TBM case is still consistent at 2σ level.

We also updated our previous analysis [19] on $\left(R_{ij} \cdot U \cdot R_{kl}\right)$ PMNS matrices for new mixing data. To draw the comparison, we found (χ^2_{min}, Best fit level) for different mixing cases [19] using old mixing data [12] and compared it with new obtained values. The corresponding results are given in Table 6. In all allowed cases, except $\left(R_{12} \cdot U_{BM} \cdot R_{13},\ R_{23} \cdot U_{TBM} \cdot R_{13}\right.$ and $\left.R_{13} \cdot U_{TBM} \cdot R_{13}\right)$, minimum χ^2 value increases which imply fitting gets tougher for those cases. With further improvement of accuracy on mixing angles, many cases might be ruled out completely.

This completes our discussion on checking the consistency of various perturbative rotations with neutrino mixing data. This study might turn out to be useful in restricting vast number of possible models which offers different corrections to these mixing schemes in neutrino model building physics. It thus can be a guideline for neutrino model building. However all such issues including the origin of these perturbations are left for future investigations.

Acknowledgements

The author acknowledges the support provided by CERN ROOT group for data plotting. He is also grateful to anonymous reviewer for making useful comments which helped in improving the manuscript.

Appendix A. Results: summary

In this appendix, we summarized all our results for easy reference on discussed rotation schemes. We also updated our previous analysis [19] with new mixing data which was done for $\left(R_{ij} \cdot U \cdot R_{kl}\right)$ rotation scheme.

In Table 4, we presented our result corresponding to $\left(R_{ij} \cdot U,\ U \cdot R_{ij}\right)$ PMNS matrices. Table 5 and Table 6 contains the results corresponding to $\left(R_{ij} \cdot R_{kl} \cdot U,\ U \cdot R_{ij} \cdot R_{kl}\right)$ and $\left(R_{ij} \cdot U \cdot R_{kl}\right)$ PMNS matrices respectively.

Table 4
(χ^2_{min}, Best fit level) for perturbation schemes that are dictated by $\left(R_{ij} \cdot U,\ U \cdot R_{ij}\right)$ PMNS matrices.

$R^l_{ij} \cdot U$				$U \cdot R^r_{ij}$			
R^l_{ij}	BM	DC	TBM	R^r_{ij}	BM	DC	TBM
R^l_{12}	(24.0, 3σ)	(204.7, $\times$)	(45.0, $\times$)	R^r_{12}	(960.7, $-$)	(1123.6, $-$)	(960.7, $-$)
R^l_{13}	(34.3, 3σ)	(202.6, $\times$)	(55.0, $\times$)	R^r_{13}	(183.3, $\times$)	(196.5, $\times$)	(9.6, 3σ)
R^l_{23}	(1094.7, $-$)	(1094.7, $-$)	(948.2, $-$)	R^r_{23}	(151.1, $\times$)	(162.9, $\times$)	(52.2, $\times$)

Table 5
(χ^2_{min}, Best fit level) for rotation schemes that are governed by $\left(R_{ij} \cdot R_{kl} \cdot U,\ U \cdot R_{ij} \cdot R_{kl}\right)$ PMNS matrices.

$R^l_{ij} \cdot R^l_{kl} \cdot U$				$U \cdot R^r_{ij} \cdot R^r_{kl}$			
$R^l_{ij} \cdot R^l_{kl}$	BM	DC	TBM	$R^r_{ij} \cdot R^r_{kl}$	BM	DC	TBM
$R^l_{12} \cdot R^l_{13}$	(13.0, 3σ)	(173.1, $\times$)	(13.9, 3σ)	$R^r_{12} \cdot R^r_{13}$	(**1.1**, **1**σ)	(65.8, 3σ)	(**1.7**, **1**σ)
$R^l_{12} \cdot R^l_{23}$	(4.4, 2σ)	(4.4, 2σ)	(41.0, $\times$)	$R^r_{12} \cdot R^r_{23}$	(50.8, $\times$)	(**1.3**, **1**σ)	(50.9, $\times$)
$R^l_{13} \cdot R^l_{12}$	(8.8, 3σ)	(140.0, $\times$)	(18.2, 3σ)	$R^r_{13} \cdot R^r_{12}$	(15.5, $\times$)	(28.0, 3σ)	(2.6, 2σ)
$R^l_{13} \cdot R^l_{23}$	(21.0, 3σ)	(21.0, 3σ)	(19.7, $\times$)	$R^r_{13} \cdot R^r_{23}$	(137.1, $\times$)	(138.4, $\times$)	(3.0, 2σ)
$R^l_{23} \cdot R^l_{12}$	(11.5, 3σ)	(35.4, $\times$)	(32.3, $\times$)	$R^r_{23} \cdot R^r_{12}$	(15.5, $\times$)	(28.0, 3σ)	(50.4, $\times$)
$R^l_{23} \cdot R^l_{13}$	(11.5, 3σ)	(**0.02**, **1**σ)	(32.3, $\times$)	$R^r_{23} \cdot R^r_{13}$	(146.6, $\times$)	(107.8, $\times$)	(5.2, 2σ)

Table 6
A comparison of (χ^2_{min}, Best fit level) for perturbation scheme that are dictated by $\left(R_{ij} \cdot U \cdot R_{kl}\right)$ PMNS matrix with previous results [19]. Since previous mixing data [12] have two regions of θ_{23} so here we mentioned best fit among those two possibilities.

$(\chi^2_{min}[R^l_{ij} \cdot U \cdot R^r_{kl}])_{Old} \rightarrow (\chi^2_{min}[R^l_{ij} \cdot U \cdot R^r_{kl}])_{New}$			
$R^l_{ij} - R^r_{kl}$	BM	DC	TBM
$R^l_{12} - R^r_{13}$	(1.4, 1σ) $\rightarrow$ (**0.8**, **1**σ)	(0.8, 1σ) $\rightarrow$ (6.3, 2σ)	(0.8, 1σ) $\rightarrow$ (6.3, 2σ)
$R^l_{12} - R^r_{23}$	(0.1, 1σ) $\rightarrow$ (23.2, 3σ)	(51.5, $\times$) $\rightarrow$ (147.9, $\times$)	(8.7, 2σ) $\rightarrow$ (13.8, 3σ)
$R^l_{13} - R^r_{12}$	(10.1, 3σ) $\rightarrow$ (22.8, 3σ)	(16.7, $\times$) $\rightarrow$ (202.6, $\times$)	(10.1, 3σ) $\rightarrow$ (22.8, 3σ)
$R^l_{13} - R^r_{23}$	(0.03, 1σ) $\rightarrow$ (**0.3**, **1**σ)	(11.7, 2σ) $\rightarrow$ (26.0, 3σ)	(11.7, 2σ) $\rightarrow$ (26.0, 3σ)
$R^l_{23} - R^r_{12}$	(93.3, $-$) $\rightarrow$ (943.3, $-$)	(93.3, $-$) $\rightarrow$ (943.3, $-$)	(93.3, $-$) $\rightarrow$ (943.3, $-$)
$R^l_{23} - R^r_{13}$	(278.5, $\times$) $\rightarrow$ (168.1, $\times$)	(278.5, $\times$) $\rightarrow$ (168.1, $\times$)	(9.7, 3σ) $\rightarrow$ (7.0, 3σ)
$R^l_{12} - R^r_{12}$	(5.9, 2σ) $\rightarrow$ (12.6, 3σ)	(9.1, 3σ) $\rightarrow$ (169.4, $\times$)	(5.9, 2σ) $\rightarrow$ (12.6, 3σ)
$R^l_{13} - R^r_{13}$	(3.6, 2σ) $\rightarrow$ (34.3, 3σ)	(12.2, 3σ) $\rightarrow$ (148.4, $\times$)	(0.2, 1σ) $\rightarrow$ (**0.2**, **1**σ)
$R^l_{23} - R^r_{23}$	(220.1, $\times$) $\rightarrow$ (135.4, $\times$)	(220.2, $\times$) $\rightarrow$ (135.4, $\times$)	(1.5, 2σ) $\rightarrow$ (1.7, 2σ)

References

[1] F.P. An, et al., DAYA-BAY Collaboration, Observation of electron-antineutrino disappearance at Daya Bay, Phys. Rev. Lett. 108 (2012) 171803, arXiv:1203.1669 [hep-ex].

[2] K. Abe, et al., T2K Collaboration, Phys. Rev. Lett. 107 (2011) 041801, arXiv:1106.2822 [hep-ex].

[3] Y. Abe, et al., DOUBLE-CHOOZ Collaboration, Indication for the disappearance of reactor electron antineutrinos in the Double Chooz experiment, Phys. Rev. Lett. 108 (2012) 131801, arXiv:1112.6353 [hep-ex].

[4] P. Adamson, et al., MINOS Collaboration, Improved search for muon-neutrino to electron-neutrino oscillations in MINOS, Phys. Rev. Lett. 107 (2011) 181802, arXiv:1108.0015 [hep-ex].

[5] J.K. Ahn, et al., RENO Collaboration, Observation of reactor electron antineutrino disappearance in the RENO experiment, Phys. Rev. Lett. 108 (2012) 191802, arXiv:1204.0626 [hep-ex].

[6] P. Minkowski, Phys. Lett. B 67 (1977) 421;
M. Gell-Mann, P. Ramond, R. Slansky, Conf. Proc. C 790927 (1979) 315, arXiv:1306.4669 [hep-th];
T. Yanagida, Conf. Proc. C 7902131 (1979) 95;
R.N. Mohapatra, G. Senjanovic, Phys. Rev. Lett. 44 (1980) 912.

[7] I. Stancu, D.V. Ahluwalia, L/E flatness of the electron – like event ratio in Super-Kamiokande and a degeneracy in neutrino masses, Phys. Lett. B 460 (1999) 431, arXiv:hep-ph/9903408;
P.F. Harrison, D.H. Perkins, W.G. Scott, Tri-bimaximal mixing and the neutrino oscillation data, Phys. Lett. B 530 (2002) 167, arXiv:hep-ph/0202074;
P.F. Harrison, W.G. Scott, Symmetries and generalisations of tri-bimaximal neutrino mixing, Phys. Lett. B 535 (2002) 163, arXiv:hep-ph/0203209;
Zhi zhong Xing, Nearly tri-bimaximal neutrino mixing and CP violation, Phys. Lett. B 533 (2002) 85, arXiv:hep-ph/0204049;
G. Altarelli, F. Feruglio, L. Merlo, E. Stamou, Discrete flavour groups, θ_{13} and lepton flavour violation, J. High Energy Phys. 1208 (2012) 021, arXiv:1205.4670 [hep-ph].

[8] F. Vissani, A study of the scenario with nearly degenerate Majorana neutrinos, arXiv:hep-ph/9708483;
V.D. Barger, S. Pakvasa, T.J. Weiler, K. Whisnant, Bi-maximal mixing of three neutrinos, Phys. Lett. B 467 (1998) 107, arXiv:hep-ph/9806387;
A.J. Baltz, A.S. Goldhaber, M. Goldhaber, The solar neutrino puzzle: an oscillation solution with maximal neutrino mixing, Phys. Rev. Lett. 81 (1998) 5730, arXiv:hep-ph/9806540;
D.V. Ahluwalia, Reconciling Super-Kamiokande, LSND, and home-stake neutrino oscillation data, Mod. Phys. Lett. A 13 (1998) 2249, arXiv:hep-ph/9807267;
H.J. He, D.A. Dicus, J.N. Ng, Phys. Lett. B 536 (2002) 83, arXiv:hep-ph/0203237;
G. Altarelli, F. Feruglio, L. Merlo, Revisiting bimaximal neutrino mixing in a model with S(4) discrete symmetry, J. High Energy Phys. 0905 (2009) 020, arXiv:0903.1940 [hep-ph];
H.J. He, X.J. Xu, Phys. Rev. D 86 (2012) 111301, arXiv:1203.2908 [hep-ph].

[9] H. Fritzsch, Z.-Z. Xing, Lepton mass hierarchy and neutrino oscillations, Phys. Lett. B 372 (1996) 265, arXiv:hep-ph/9509389;
H. Fritzsch, Z.-z. Xing, Large leptonic flavor mixing and the mass spectrum of leptons, Phys. Lett. B 440 (1998) 313, arXiv:hep-ph/9808272.

[10] K.S. Babu, E. Ma, J.W.F. Valle, Underlying A(4) symmetry for the neutrino mass matrix and the quark mixing matrix, Phys. Lett. B 552 (2003) 207, arXiv:hep-ph/0206292;
A. Zee, Obtaining the neutrino mixing matrix with the tetrahedral group, Phys. Lett. B 630 (2005) 58, arXiv:hep-ph/0508278;
E. Ma, Tetrahedral family symmetry and the neutrino mixing matrix, Mod. Phys. Lett. A 20 (2005) 2601, arXiv:hep-ph/0508099;
B. Adhikary, B. Brahmachari, A. Ghosal, E. Ma, M.K. Parida, A(4) symmetry and prediction of U(e3) in a modified Altarelli–Feruglio model, Phys. Lett. B 638 (2006) 345, arXiv:hep-ph/0603059;
G. Altarelli, F. Feruglio, L. Merlo, Tri-bimaximal neutrino mixing and discrete flavour symmetries, arXiv:1205.5133 [hep-ph];
G. Altarelli, F. Feruglio, Discrete flavor symmetries and models of neutrino mixing, Rev. Mod. Phys. 82 (2010) 2701, arXiv:1002.0211 [hep-ph];
S.F. King, C. Luhn, Neutrino mass and mixing with discrete symmetry, Rep. Prog. Phys. 76 (2013) 056201, arXiv:1301.1340 [hep-ph];
H. Ishimori, T. Kobayashi, H. Ohki, Y. Shimizu, H. Okada, M. Tanimoto, Non-Abelian discrete symmetries in particle physics, Prog. Theor. Phys. Suppl. 183 (2010) 1, arXiv:1003.3552 [hep-th].

[11] E. Ma, Neutrino mass matrix from S(4) symmetry, Phys. Lett. B 632 (2006) 352, arXiv:hep-ph/0508231;
C.S. Lam, The unique horizontal symmetry of leptons, Phys. Rev. D 78 (2008) 073015, arXiv:0809.1185 [hep-ph];
C.S. Lam, A horizontal symmetry for leptons and quarks, arXiv:1105.4622 [hep-ph].

[12] M.C. Gonzalez-Garcia, M. Maltoni, T. Schwetz, J. High Energy Phys. 1411 (2014) 052, arXiv:1409.5439 [hep-ph].

[13] F. Capozzi, E. Di Valentino, E. Lisi, A. Marrone, A. Melchiorri, A. Palazzo, Phys. Rev. D 95 (9) (2017) 096014, https://doi.org/10.1103/PhysRevD.95.096014, arXiv:1703.04471 [hep-ph].

[14] S. Zhou, Relatively large θ_{13} and nearly maximal θ_{23} from the approximate S_3 symmetry of lepton mass matrices, Phys. Lett. B 704 (2011) 291, arXiv:1106.4808 [hep-ph];
T. Araki, Getting at large θ_{13} with almost maximal θ_{23} from tri-bimaximal mixing, Phys. Rev. D 84 (2011) 037301, arXiv:1106.5211 [hep-ph];
H. Zhang, S. Zhou, Radiative corrections and explicit perturbations to the tetra-maximal neutrino mixing with large θ_{13}, Phys. Lett. B 704 (2011) 296, arXiv:1107.1097 [hep-ph];
W. Rodejohann, H. Zhang, S. Zhou, Systematic search for successful lepton mixing patterns with nonzero θ_{13}, Nucl. Phys. B 855 (2012) 592, arXiv:1107.3970 [hep-ph];
S. Antusch, S.F. King, C. Luhn, M. Spinrath, Trimaximal mixing with predicted θ_{13} from a new type of constrained sequential dominance, Nucl. Phys. B 856 (2012) 328, arXiv:1108.4278 [hep-ph];
S.-F. Ge, D.A. Dicus, W.W. Repko, Residual symmetries for neutrino mixing with a large θ_{13} and nearly maximal δ_D, Phys. Rev. Lett. 108 (2012) 041801, arXiv:1108.0964 [hep-ph];
P.O. Ludl, S. Morisi, E. Peinado, The reactor mixing angle and CP violation with two texture zeros in the light of T2K, Nucl. Phys. B 857 (2012) 411, arXiv:1109.3393 [hep-ph];
S.F. Ge, H.J. He, F.R. Yin, J. Cosmol. Astropart. Phys. 1005 (2010) 017, arXiv:1001.0940 [hep-ph];
H.J. He, F.R. Yin, Phys. Rev. D 84 (2011) 033009, arXiv:1104.2654 [hep-ph];
S. Dev, S. Gupta, R.R. Gautam, L. Singh, Near maximal atmospheric mixing in neutrino mass matrices with two vanishing minors, Phys. Lett. B 706 (2011) 168, arXiv:1111.1300 [hep-ph];
R. Dutta, U. Ch, A.K. Giri, N. Sahu, Perturbative bottom-up approach for neutrino mass matrix in light of large θ_{13} and role of lightest neutrino mass, arXiv:1303.3357 [hep-ph];
D.V. Ahluwalia, CP violating tri-bimaximal-Cabibbo mixing, ISRN High Energy Phys. 2012 (2012) 954272, arXiv:1206.4779 [hep-ph];
Y. Shimizu, R. Takahashi, M. Tanimoto, Minimal neutrino texture with neutrino mass ratio and Cabibbo angle, PTEP 2013 (6) (2013) 063B02, arXiv:1212.5913 [hep-ph];
D. Borah, arXiv:1307.2426 [hep-ph];
W. Rodejohann, H. Zhang, arXiv:1402.2226 [hep-ph];
D. Zhuridov, arXiv:1304.4870 [hep-ph];
J. Kile, M.J. Pérez, P. Ramond, J. Zhang, Phys. Rev. D 90 (1) (2014) 013004, arXiv:1403.6136 [hep-ph];
D. Zhuridov, arXiv:1405.5522 [hep-ph];
S.T. Petcov, Nucl. Phys. B 892 (2015) 400, arXiv:1405.6006 [hep-ph];
S.K. Kang, C.S. Kim, Phys. Rev. D 90 (7) (2014) 077301, arXiv:1406.5014 [hep-ph];
I. Girardi, S.T. Petcov, A.V. Titov, Nucl. Phys. B 894 (2015) 733, arXiv:1410.8056 [hep-ph];
A. Damanik, arXiv:1505.00681 [hep-ph];
Z.z. Xing, Z.h. Zhao, Rep. Prog. Phys. 79 (7) (2016) 076201, arXiv:1512.04207 [hep-ph];
J. Zhang, S. Zhou, J. High Energy Phys. 1609 (2016) 167, arXiv:1606.09591 [hep-ph].

[15] Y. Shimizu, M. Tanimoto, A. Watanabe, Breaking tri-bimaximal mixing and large θ_{13}, Prog. Theor. Phys. 126 (2011) 81, arXiv:1105.2929 [hep-ph];
A.S. Joshipura, K.M. Patel, Viability of the exact tri-bimaximal mixing at M_{GUT} in SO(10), J. High Energy Phys. 1109 (2011) 137, arXiv:1105.5943 [hep-ph];
S. Morisi, K.M. Patel, E. Peinado, Model for T2K indication with maximal atmospheric angle and tri-maximal solar angle, Phys. Rev. D 84 (2011) 053002, arXiv:1107.0696 [hep-ph];
P.S. Bhupal Dev, R.N. Mohapatra, M. Severson, Neutrino mixings in SO(10) with type II seesaw and θ_{13}, Phys. Rev. D 84 (2011) 053005, arXiv:1107.2378 [hep-ph];
R.d.A. Toorop, F. Feruglio, C. Hagedorn, Discrete flavour symmetries in light of T2K, Phys. Lett. B 703 (2011) 447, arXiv:1107.3486 [hep-ph];
A. Adulpravitchai, R. Takahashi, A4 flavor models in split seesaw mechanism, J. High Energy Phys. 1109 (2011) 127, arXiv:1107.3829 [hep-ph];
A. Rashed, A. Datta, The charged lepton mass matrix and non-zero θ_{13} with TeV scale new physics, Phys. Rev. D 85 (2012) 035019, arXiv:1109.2320 [hep-ph];

S. Gupta, A.S. Joshipura, K.M. Patel, Minimal extension of tri-bimaximal mixing and generalized $Z_2 X Z_2$ symmetries, Phys. Rev. D 85 (2012) 031903, arXiv:1112.6113 [hep-ph];
S.F. King, C. Luhn, A4 models of tri-bimaximal-reactor mixing, J. High Energy Phys. 1203 (2012) 036, arXiv:1112.1959 [hep-ph];
P.S. Bhupal Dev, B. Dutta, R.N. Mohapatra, M. Severson, θ_{13} and proton decay in a minimal $SO(10) \times S_4$ model of flavor, Phys. Rev. D 86 (2012) 035002, arXiv:1202.4012 [hep-ph].

[16] Z.-Z. Xing, The T2K indication of relatively large θ_{13} and a natural perturbation to the democratic neutrino mixing pattern, Chin. Phys. C 36 (2012) 101, arXiv:1106.3244 [hep-ph].

[17] X.-G. He, A. Zee, Minimal modification to the tri-bimaximal neutrino mixing, Phys. Lett. B 645 (2007) 427, arXiv:hep-ph/0607163;
C.H. Albright, W. Rodejohann, Comparing trimaximal mixing and its variants with deviations from tri-bimaximal mixing, Eur. Phys. J. C 62 (2009) 599, arXiv:0812.0436 [hep-ph];
C.H. Albright, A. Dueck, W. Rodejohann, Possible alternatives to tri-bimaximal mixing, Eur. Phys. J. C 70 (2010) 1099, arXiv:1004.2798 [hep-ph];
X.-G. He, A. Zee, Minimal modification to tri-bimaximal mixing, Phys. Rev. D 84 (2011) 053004, arXiv:1106.4359 [hep-ph].

[18] W. Chao, Y.-j. Zheng, Relatively large θ_{13} from modification to the tri-bimaximal, bimaximal and democratic neutrino mixing matrices, J. High Energy Phys. 1302 (2013) 044, arXiv:1107.0738 [hep-ph].

[19] S.K. Garg, S. Gupta, J. High Energy Phys. 1310 (2013) 128, arXiv:1308.3054 [hep-ph].

[20] B. Pontecorvo, Zh. Eksp. Teor. Fiz. (JTEP) 33 (1957) 549;
B. Pontecorvo, Zh. Eksp. Teor. Fiz. (JTEP) 34 (1958) 247;
B. Pontecorvo, Zh. Eksp. Teor. Fiz. (JTEP) 53 (1967) 1717;
Z. Maki, M. Nakagawa, S. Sakata, Prog. Theor. Phys. 28 (1962) 870.

[21] G. Altarelli, F. Feruglio, I. Masina, Can neutrino mixings arise from the charged lepton sector?, Nucl. Phys. B 689 (2004) 157, arXiv:hep-ph/0402155;
A. Romanino, Charged lepton contributions to the solar neutrino mixing and θ_{13}, Phys. Rev. D 70 (2004) 013003, arXiv:hep-ph/0402258;
S. Antusch, S.F. King, Charged lepton corrections to neutrino mixing angles and CP phases revisited, Phys. Lett. B 631 (2005) 42, arXiv:hep-ph/0508044;
J.C. Gomez-Izquierdo, A. Perez-Lorenzana, Phys. Rev. D 77 (2008) 113015, arXiv:0711.0045 [hep-ph];
J.C. Gomez-Izquierdo, A. Perez-Lorenzana, Phys. Rev. D 82 (2010) 033008, arXiv:0912.5210 [hep-ph];
D. Marzocca, S.T. Petcov, A. Romanino, M. Spinrath, Sizeable θ_{13} from the charged lepton sector in SU(5), (tri-)bimaximal neutrino mixing and Dirac CP violation, J. High Energy Phys. 1111 (2011) 009, arXiv:1108.0614 [hep-ph];
S. Dev, S. Gupta, R.R. Gautam, Parametrizing the lepton mixing matrix in terms of charged lepton corrections, Phys. Lett. B 704 (2011) 527, arXiv:1107.1125 [hep-ph];
D. Marzocca, S.T. Petcov, A. Romanino, M.C. Sevilla, Nonzero $|U_e 3|$ from charged lepton corrections and the atmospheric neutrino mixing angle, J. High Energy Phys. 1305 (2013) 073, arXiv:1302.0423 [hep-ph];
S. Dev, R.R. Gautam, L. Singh, Phys. Rev. D 89 (2014) 013006, arXiv:1309.4219 [hep-ph];
D. Zhuridov, arXiv:1304.4870 [hep-ph];
J.C. Gómez-Izquierdo, Eur. Phys. J. C 77 (8) (2017) 551, arXiv:1701.01747 [hep-ph];
J.C. Gómez-Izquierdo, F. Gonzalez-Canales, M. Mondragón, Int. J. Mod. Phys. A 32 (28–29) (2017) 1750171, arXiv:1705.06324 [hep-ph].

[22] S. Pakvasa, W. Rodejohann, T.J. Weiler, Unitary parametrization of perturbations to tribimaximal neutrino mixing, Phys. Rev. Lett. 100 (2008) 111801, arXiv:0711.0052 [hep-ph];
S.M. Boucenna, S. Morisi, M. Tortola, J.W.F. Valle, Bi-large neutrino mixing and the Cabibbo angle, Phys. Rev. D 86 (2012) 051301, arXiv:1206.2555 [hep-ph];
B. Hu, Neutrino mixing: perturbation, parameterization and trimaximal-Cabibbo mixing, Phys. Rev. D 87 (2013) 053011, arXiv:1212.4079 [hep-ph].

[23] H. Fritzsch, Z.-Z. Xing, Phys. Lett. B 372 (1996) 265, arXiv:hep-ph/9509389;
H. Fritzsch, Z.-z. Xing, Phys. Lett. B 440 (1998) 313, arXiv:hep-ph/9808272;
M. Fukugita, M. Tanimoto, T. Yanagida, Phys. Rev. D 57 (1998) 4429, arXiv:hep-ph/9709388;
W. Rodejohann, Z.-z. Xing, Phys. Lett. B 601 (2004) 176, arXiv:hep-ph/0408195;
T. Kitabayashi, M. Yasue, Phys. Lett. B 713 (2012) 206, arXiv:1204.4523 [hep-ph].